

## § 4. Switches

P72

\* High-power switching systems are the connecting elements between the storage device and the load.

- - rise time
- shape.
- amplitude

} of the generator output pulse depend strongly on the properties of the switches

### § 4.1 closing switches

\* the switching process is associated with voltage breakdown across an initially insulant element.

- automatically
- externally supplied trigger pulse.

#### § 4.1.1 Gas switches

- commonly applied in high-power pulse generators
- easy to use
- handle large currents
- ... charges
- ~~these~~ can be triggered precisely.

\* Many applications require a precisely controlled initiation of the ~~voltage~~ voltage breakdown.

→ The trigger method applied has a big influence on the ignition delay & its variance (jitter)

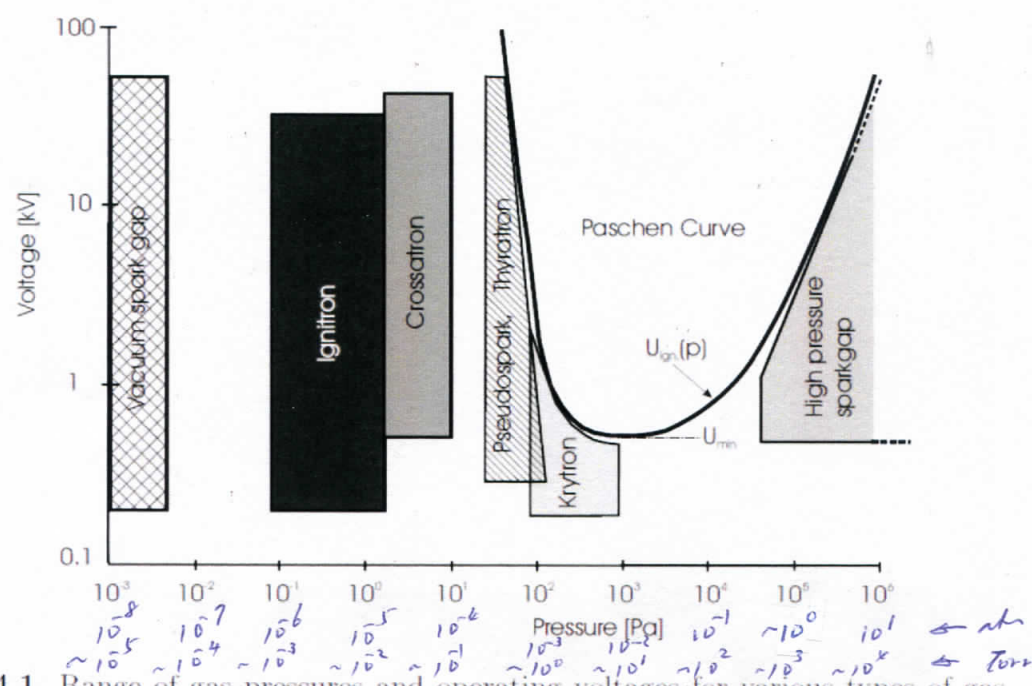


Fig. 4.1. Range of gas pressures and operating voltages for various types of gas switches. In addition, the Paschen curve for air is shown for a fixed gap width of 3 mm. Above this curve, switch operation becomes impossible since the breakdown strength is exceeded

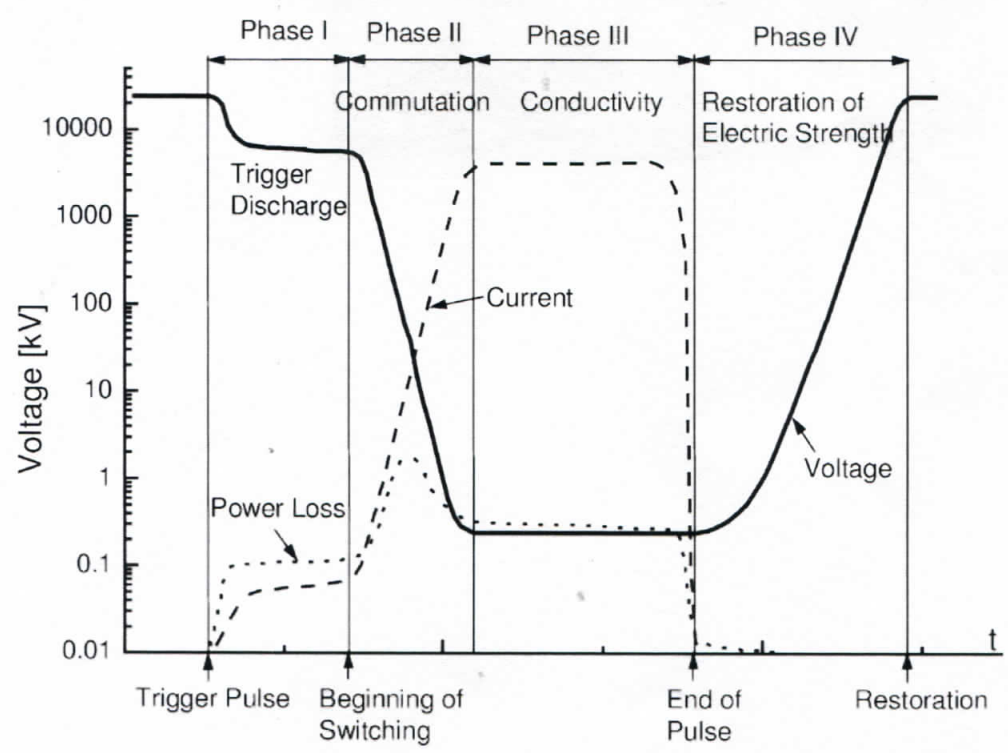


Fig. 4.2. Evolution of voltage, current, and power loss in a gas-filled switching system

→ Operation of the switch can be divided into 4 phases: p74

- 1: Trigger phase - build-up of a trigger discharge.
- 2: Transition phase / commutation  
- transition from high  $\rightarrow$  low switch impedance.
- 3: Stationary phase  
- constant conductivity
- 4: Recovery phase.  
- restoration of the previous electric strength.

\* energy loss:

$$W_V = \int_0^{T_s} U(t) \cdot I(t) \cdot dt \approx \int_0^{T_s} U_m \left(1 - \frac{t}{T_s}\right) \cdot I_m \frac{t}{T_s} dt$$
$$= U_m \cdot I_m \int_0^{T_s} \left(1 - \frac{t}{T_s}\right) \frac{t}{T_s} dt = \frac{U_m \cdot I_m \cdot T_s}{6} \approx 0.2 U_m I_m \cdot T_r$$

$T_s \rightarrow$  switching time

$T_r \rightarrow$  pulse rise time ( ~~$T_r$~~   $T_r \approx 0.8 T_s$ )

$U_m, I_m \rightarrow$  maximum voltage & current

→ need to be removed by cooling.

## 3 4.1.1.1 Gas-Filled Spark Gaps

p25

\* Break down due to:

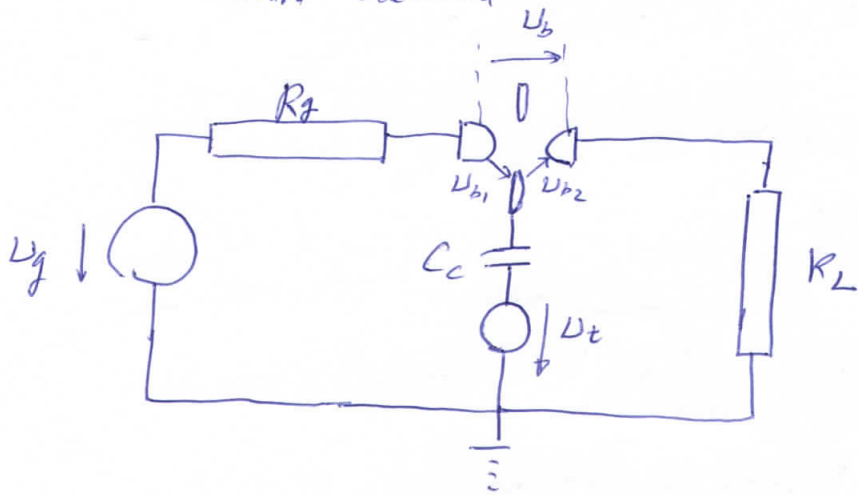
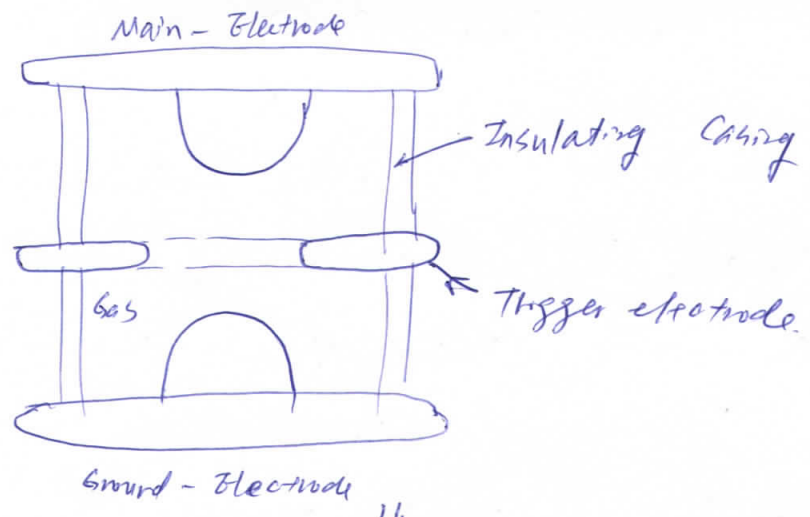
- breakdown voltage has been exceeded.
- breakdown strength has been reduced by certain events (UV radiation, plasma diffusion, etc.)

\* Important parameters:

- self-breakdown / hold-off voltage  $U_b$ .
- variance of  $U_b$   $\rightarrow$  determines the probability of breakdown.
- operation range  $\rightarrow$  range of voltage ~~held off~~  
w/ - held off w/ sufficiently low prebreakdown possibility
- reliably triggered.
- jitter
- switching time  $t_s$   $\rightarrow$  decay of the impedance (resistance & inductance)
- prebreakdown inductance & capacitance
- repetition rate capability
- lifetime & cost.

\* Triggering can be achieved by

- a laser pulse
- HV pulse.



- $U_g$ : generator voltage
- $U_b$ : breakdown voltage
- $U_t$ : trigger voltage
- $U_{b1} / U_{b2}$ : — — — — — of the partial gaps
- $R_g$ : generator impedance
- $R_L$ : Load
- $C_c$ : coupling capacitor.

- \* Longitudinal overvoltage triggering - if the voltage amplitude of the trigger pulse added to the applied operating voltage is sufficient to breakdown a partial gap.
  - \* Ignition of the 2<sup>nd</sup> partial gap occurs if its breakdown voltage is less than the operating voltage.
  - \*  $C_c \rightarrow$  used to decouple the trigger source from the generator.
- $$C_c \gg C_{b1} \Rightarrow U_{trigger}(t=0) \approx 0$$
- $$= U_g \cdot \frac{C_{b1}}{C_c + C_{b1}} \approx 0$$

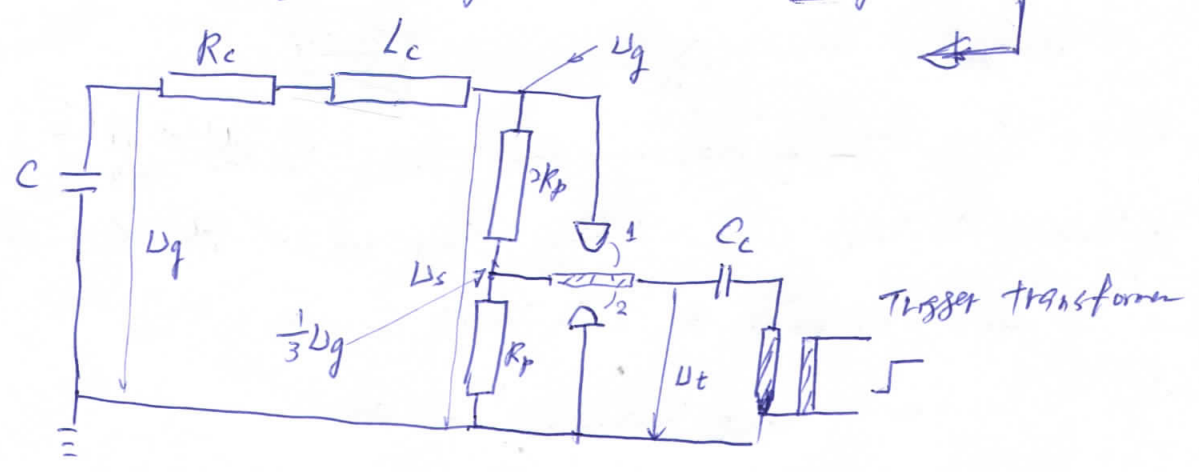
$U_g + |U_t| > U_{b1}$  ← Longitudinal overvoltage triggering  
 $|U_t| < U_{b2}$  ←  $U_t$  won't cause breakdown @  $U_{b2}$   
 $U_g > U_{b2}$  ←  
 $\rightarrow U_g \geq U_{b2} \Rightarrow U_{gmin} = U_{b2}$   
 $\rightarrow |U_{tmax}| \leq U_{b2} \Rightarrow |U_{tmax}| = U_{b2}$   
 $\rightarrow U_{gmin} + |U_{tmax}| = 2U_{b2} > U_{b1} \Rightarrow U_{b2} = \frac{1}{2}U_{b1}$   
 @ the limit.

$\Rightarrow$  For a symmetric spark gap configuration, the trigger electrode should be positioned @  $\frac{2}{3}$  of the gap spacing from the main electrode.

also  $U_g < U_{b1} = 2U_{b2}$  is needed

$\Rightarrow U_{b2} < U_g < 2U_{b2}$

or  $\frac{1}{3}U_b < U_g < \frac{2}{3}U_b \Rightarrow$  Using resistive divider:



@ Sep 1:  $\frac{2}{3}U_g < U_{b1}$

$U_g > U_{b2}$  ← when all closed, trigger pin  $\rightarrow U_g$

$U_g + |U_t| > U_{b1}$  ← when pulse come on, trigger pin  $\rightarrow U_t$

$|U_t| < U_{b2}$

$$U_g > U_{b2} \Rightarrow U_{g, \text{nom}} = U_{b2}$$

$$|U_t| < U_{b2} \Rightarrow |U_{t, \text{max}}| = U_{b2}$$

$$\Rightarrow U_g + |U_t| > U_{b1} \Rightarrow 2U_{b2} = U_{b1} \text{ (in extreme case)}$$

$$\text{(or } U_{b2} = \frac{1}{2}U_{b1}\text{)}$$

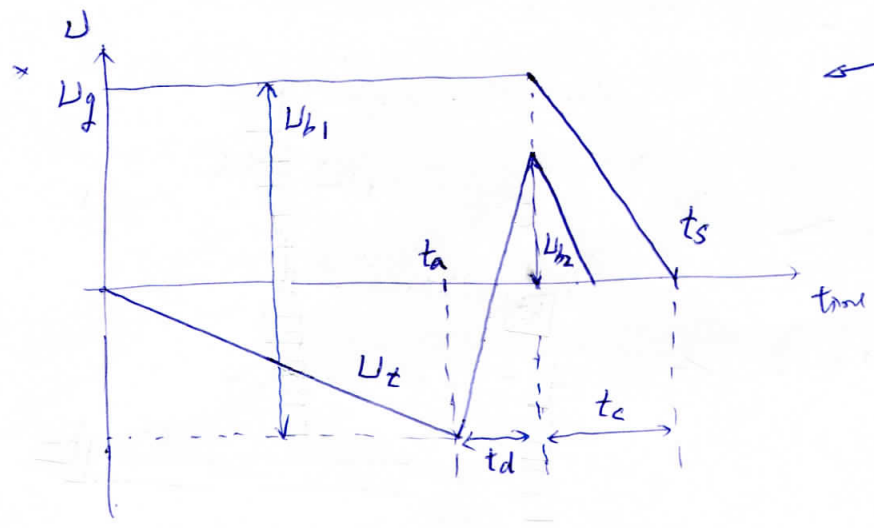
$$\frac{2}{3}U_g < U_{b1} = 2U_{b2} \Rightarrow \frac{1}{3}U_g < U_{b2} \text{ or } U_g < 3U_{b2}$$

$$\Rightarrow U_{b2} < U_g < 3U_{b2}$$

Notice that  $U_{b2} = \frac{1}{3}U_b$   
 $(\because U_b = U_{b1} + U_{b2} = 3U_{b2})$

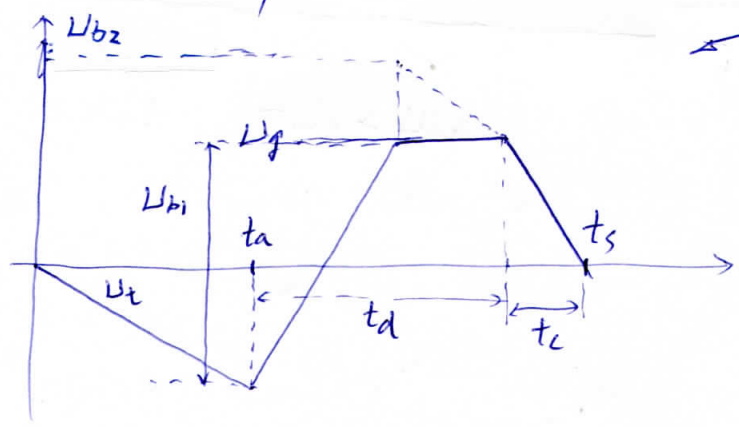
$$\Rightarrow \frac{1}{3}U_b < U_g < U_b$$

\* Show the electric field (Fig 4.6)



← longitudinal- overvoltage - triggering

- $t_a$ : trigger actuating time
- $t_d$ : switching delay
- $t_c$ : commutation time
- $t_s$ : switching time.



← longitudinal-plasma-triggering.

\* Longitudinal plasma triggering:

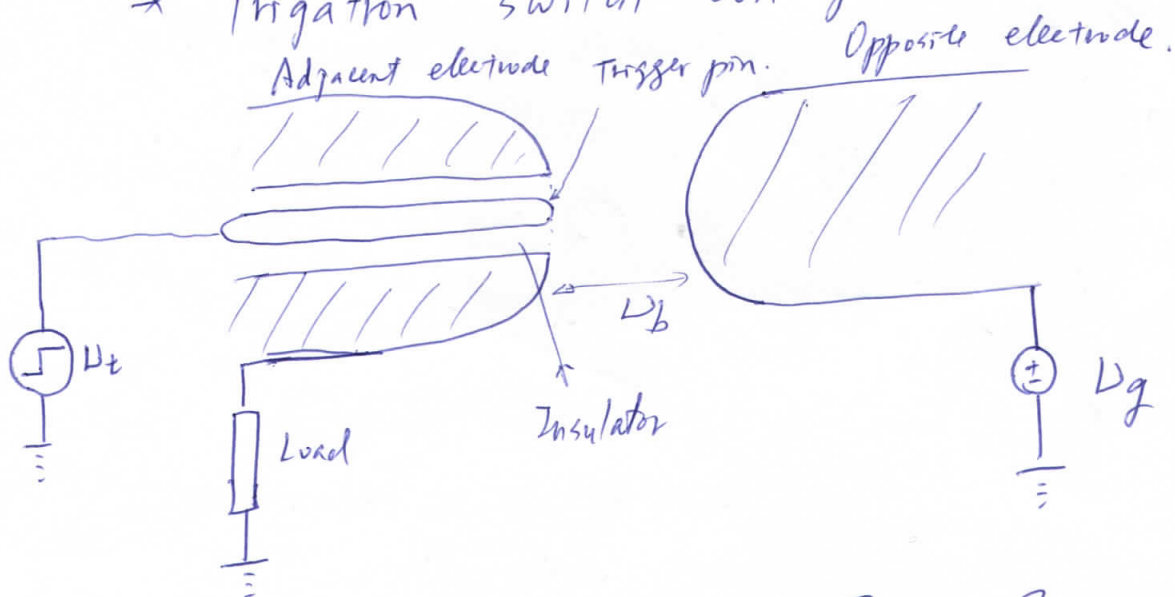
$$U_g < U_{b2}$$

⇒ 2<sup>nd</sup> gap can fire only if its breakdown strength is continuous reduced by UV radiation from the spark channel plasma of the 1<sup>st</sup> gap.

⇒ Larger switch delay time.  
much

\* Longitudinal trigger can occur only for opposite polarities of the operating and triggering voltages.

\* Triggering switch configuration.



\* Best trigger performance: Trigger & operation voltage are opposite.

n.e.  $U_t \cdot U_g < 0$

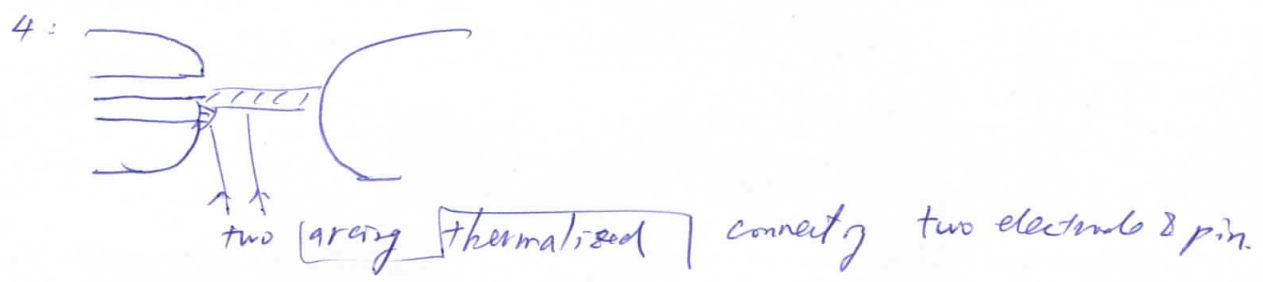
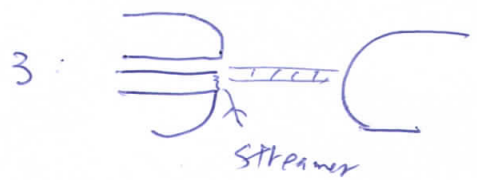
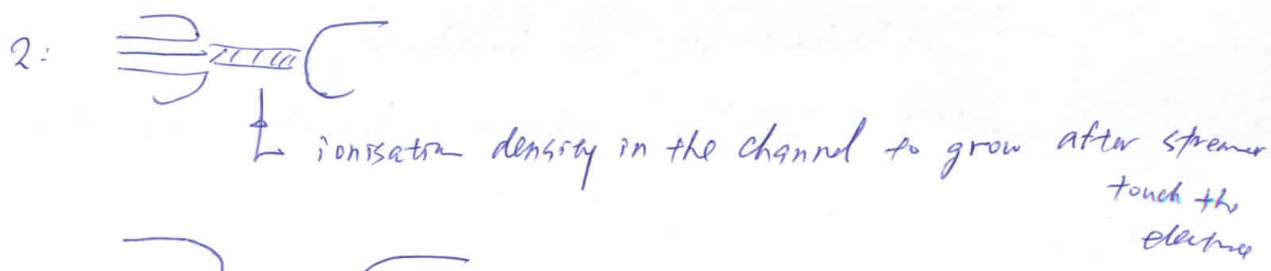
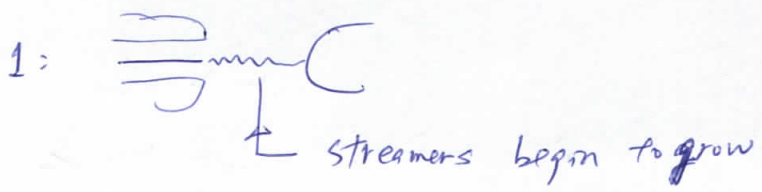
$$U_g \sim (80 - 99\%) U_b$$

$U_g \sim 50\% U_b$  is possible → large delay & jitter.

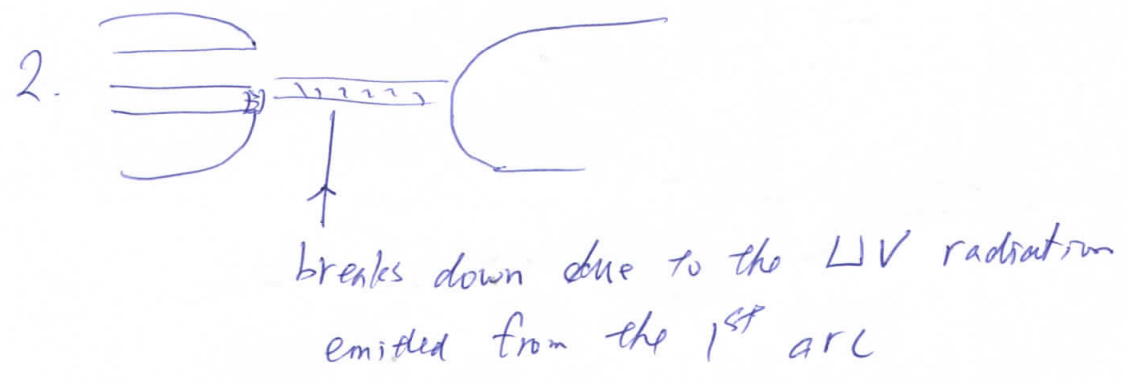
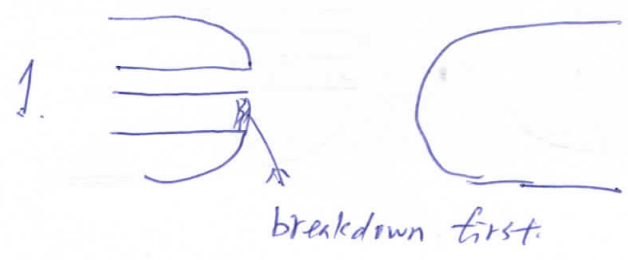


Sequence:

Case 1



Case 2:



\* Case 2: trigger pulse & the operation voltage have the same polarity.

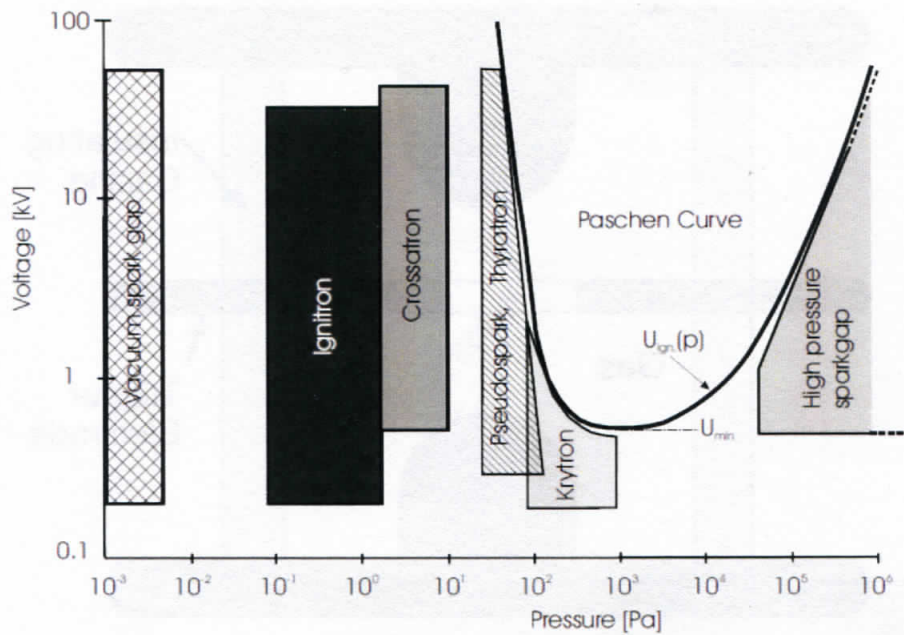


Fig. 4.1. Range of gas pressures and operating voltages for various types of gas switches. In addition, the Paschen curve for air is shown for a fixed gap width of 3 mm. Above this curve, switch operation becomes impossible since the breakdown strength is exceeded

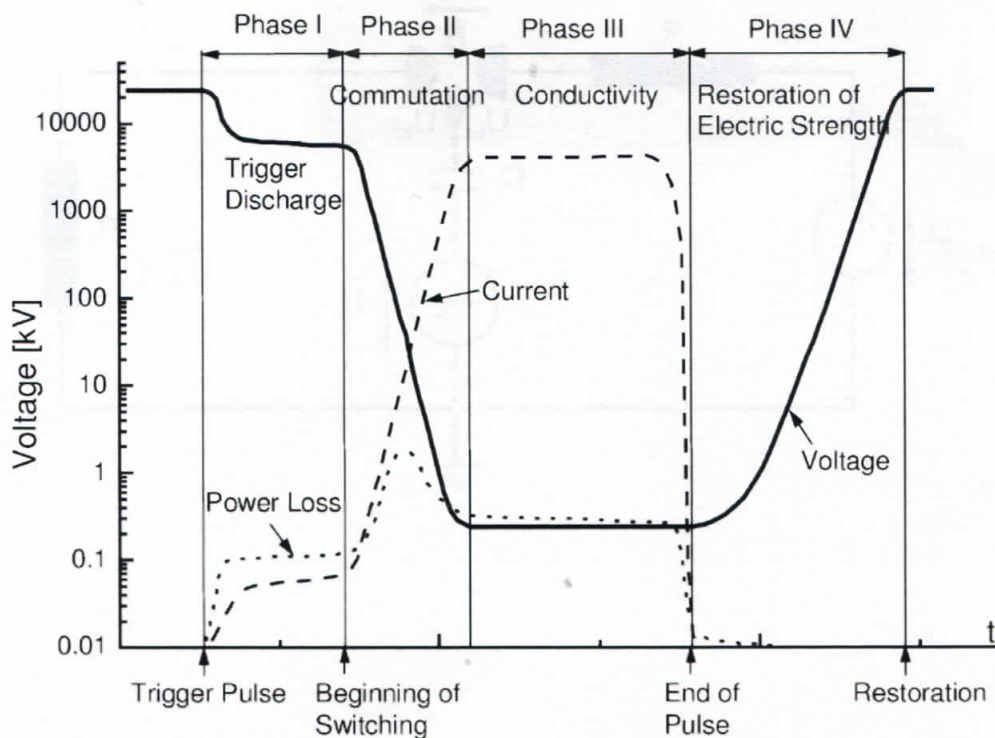


Fig. 4.2. Evolution of voltage, current, and power loss in a gas-filled switching system

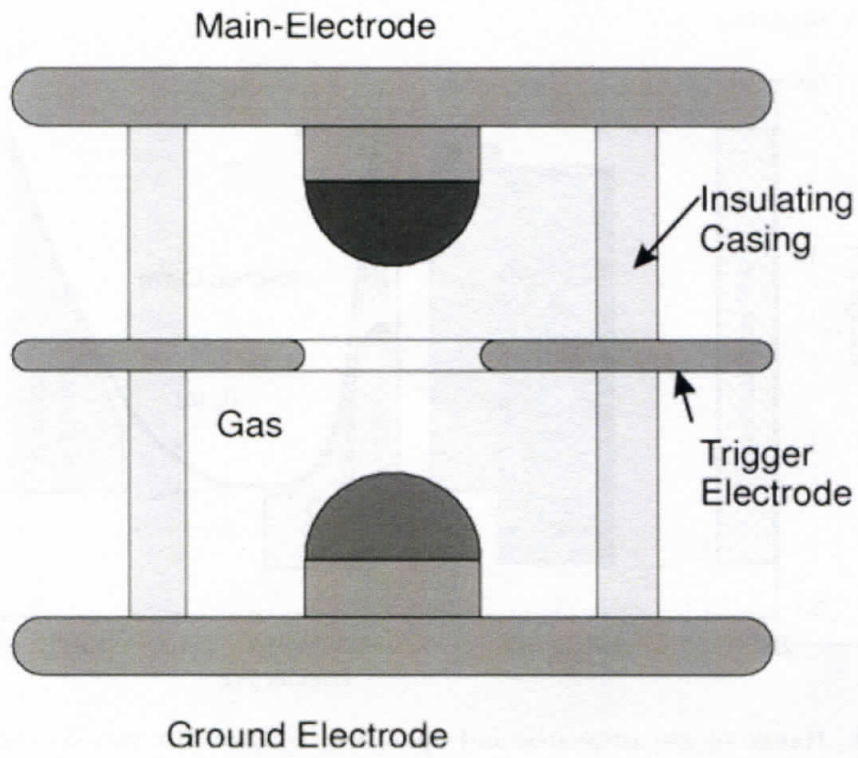
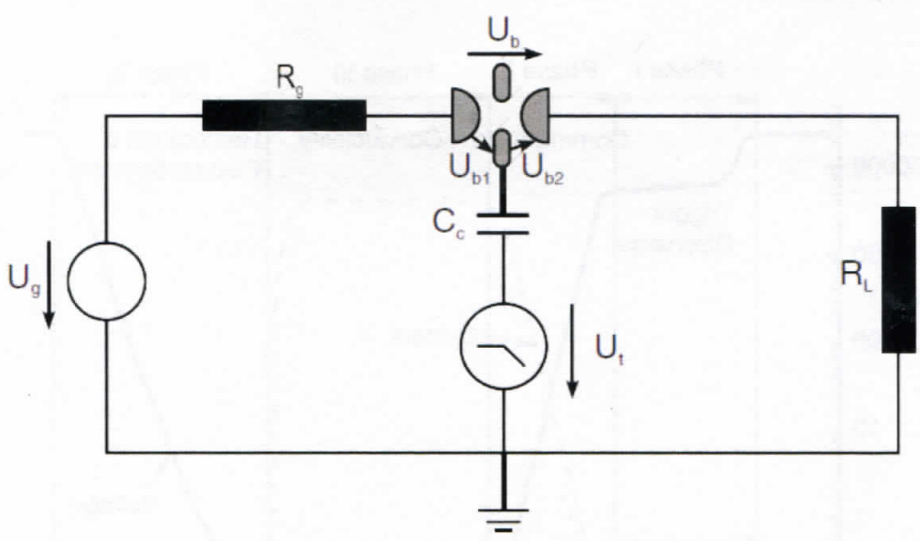
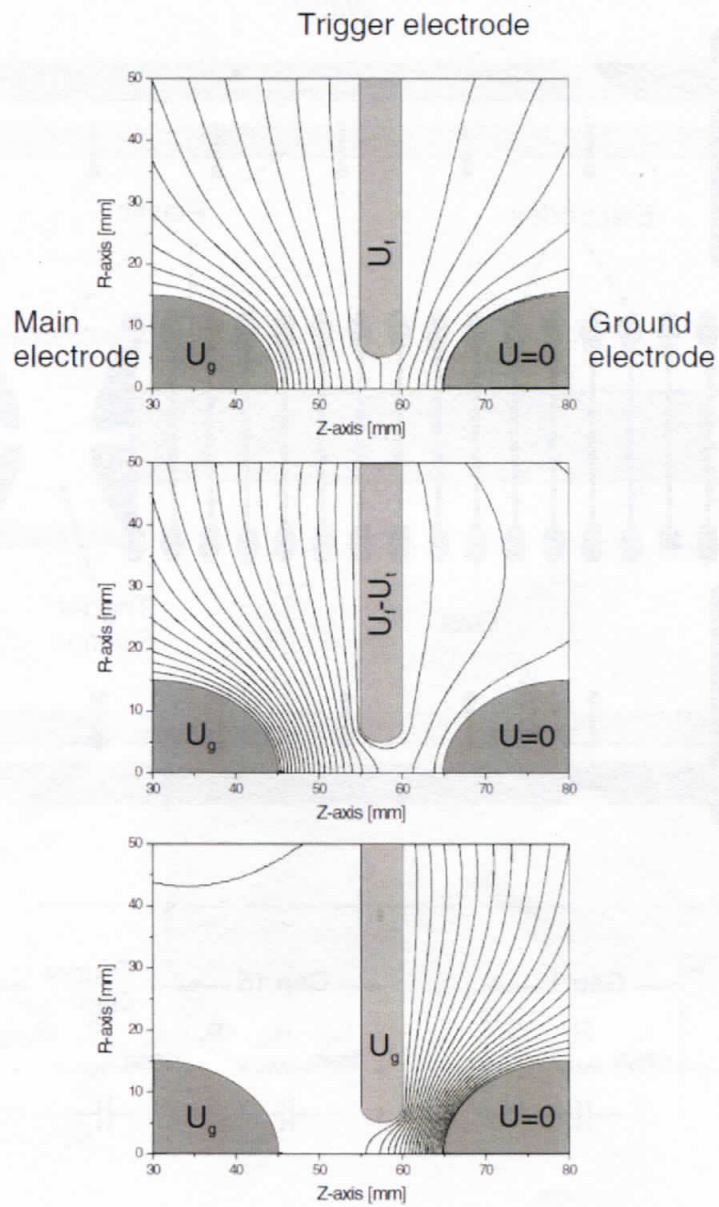


Fig. 4.3. Components of a three-electrode spark gap





**Fig. 4.6.** Potential distribution in a three-electrode spark gap switch, before ignition (*top*), after application of a trigger signal (*centre*), and after breakdown of the first gap (*bottom*)

§4.1.1.3 Multistage spark-gap switch with laser triggering

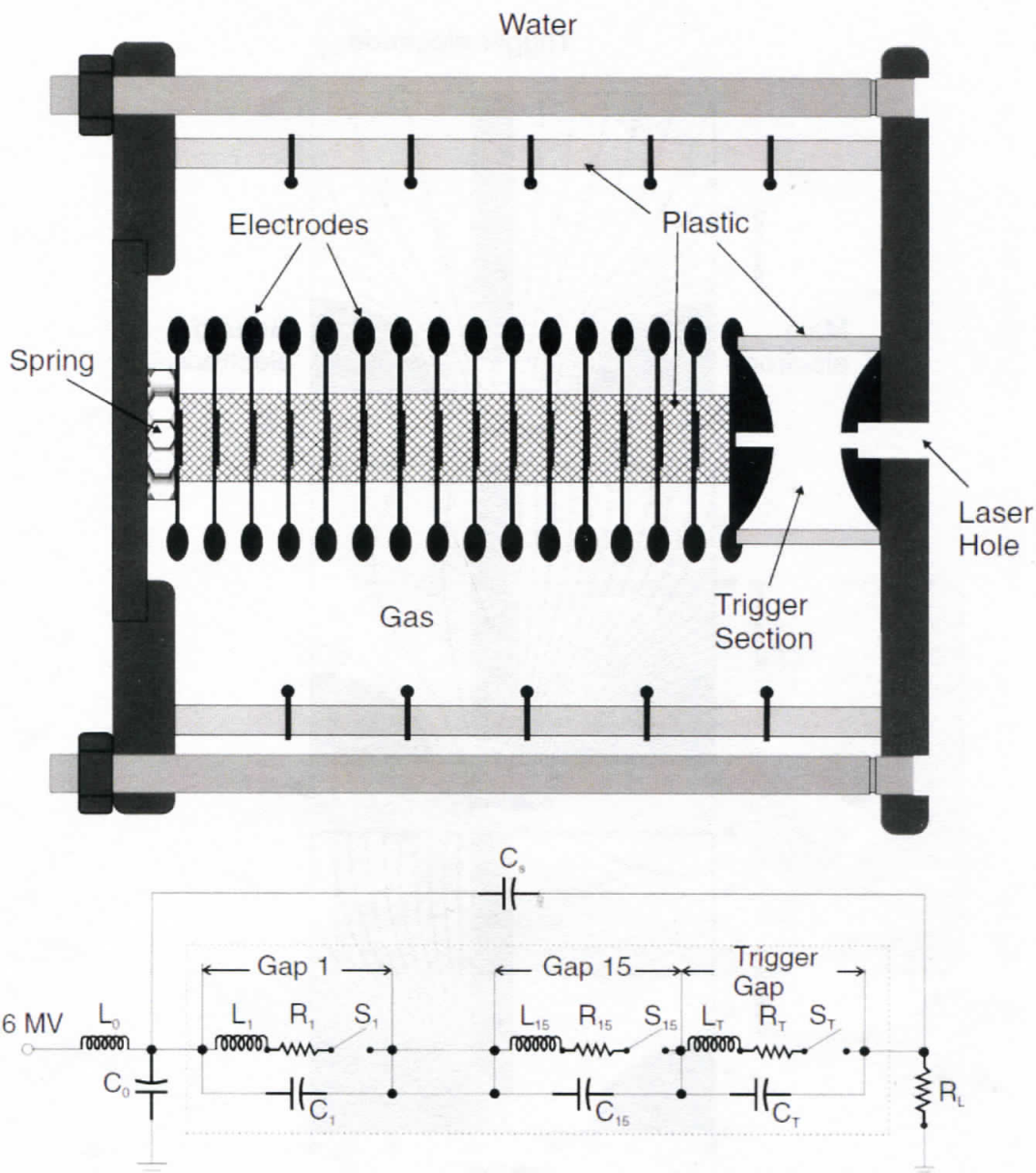


Fig. 4.12. General set-up of a high-power laser-triggered spark gap for 6 MV and 0.5 MA operating voltage and current, respectively

- Simply scaling a three-electrode spark gap to multimegavolt operating voltages would lead to large gaps, making the jitter and inductance unacceptably high.
- Operating voltage of up to 6 MV and a switch current of 0.5 MA
- It consists of 15 equal spark gaps and a trigger section.
- The operating voltage is around 90% of the self-breakdown value with a prefire probability of 0.1%.
- The gap capacitances are small, 20% of the operating voltage occurs across the trigger section.

- The switch is 68 cm long and 61 cm in diameter.
- The 1<sup>st</sup> gap is 5.7 cm and a UV laser pulse (KrF) with a 25mJ pulse energy is necessary.
- ~ 1 ns after the laser pulse, a breakdown occurs in the trigger gap and the voltage increases across the remaining gaps rapidly. An ignition wave propagates to the other gaps and ignites them sequentially.
- Total inductance: 400 nH; Trigger delay: 20 ns; jitter < 0.4 ns.

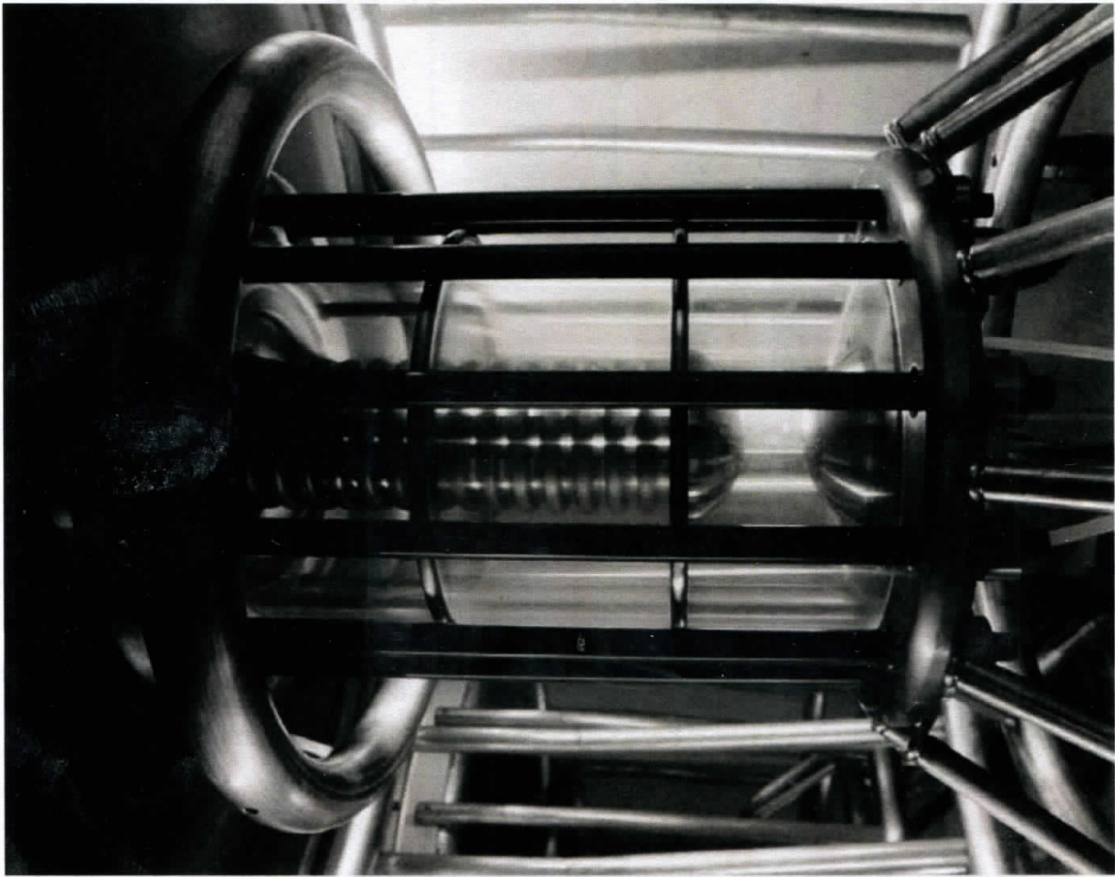


Fig. 4.13. A 4 MV version of a multigap spark switch

### §4.1.1.6 Thyratrons

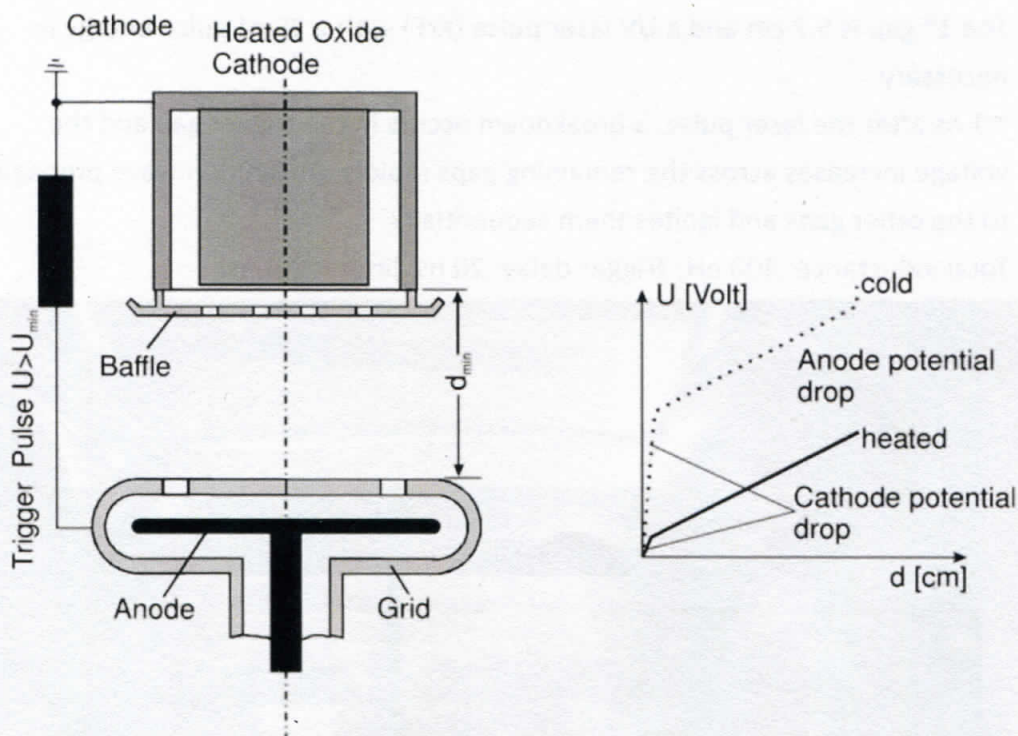
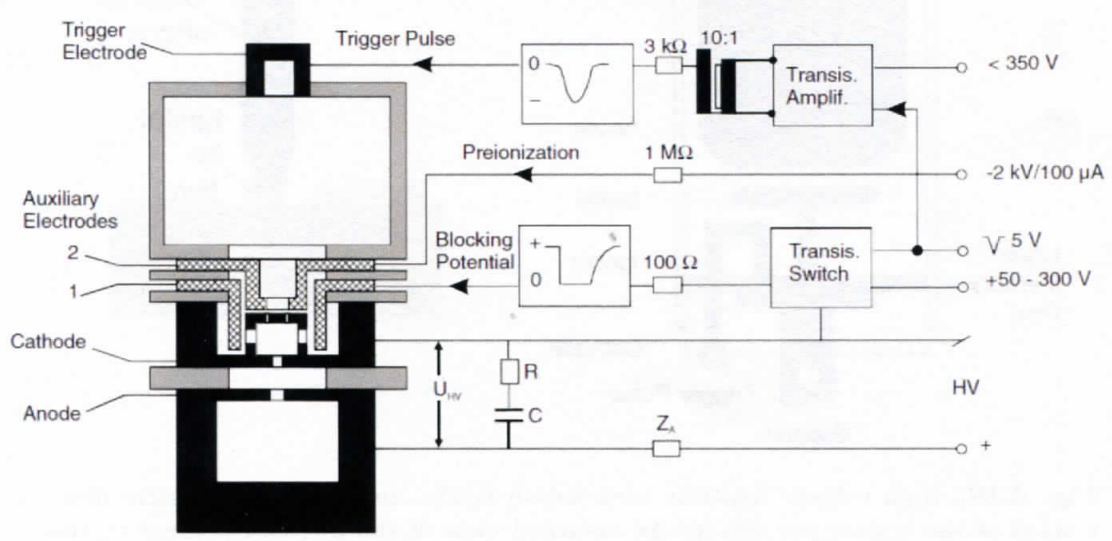
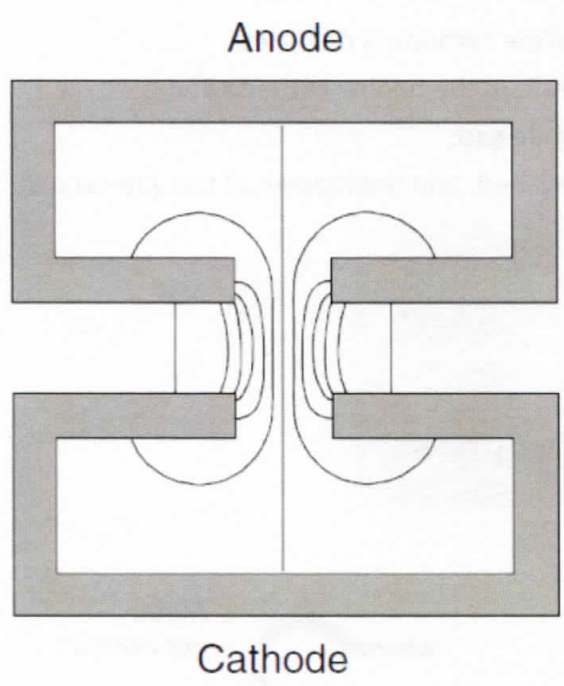


Fig. 4.15. Principal features of a thyatron with heated cathode (left), and potential drop with a heated cathode (solid line) and without one (right). The grid surrounds the anode such that the  $pd$  value excludes the possibility of a long-distance discharge

- Thyratrons are gas-filled switching devices with a gas pressure much lower than a spark-gap switches ( $30-80 \text{ Pa}/3 \times 10^{-4} - 8 \times 10^{-4} \text{ atm}$ ) and a triode configuration is used.
- The thyatron is characterized by the presence of a plasma, which allows the passage of large currents without significant electrode erosion.
- The hold-off voltage is limited by field emission,  $> 10^5 \text{ V/cm}$ .
- The anode-grid distance is 2-3 mm,  $\sim 40 \text{ kV}$  hold-off voltage.
- The cathode-grid distance corresponds to the Paschen minimum  $U_{min}$ .
- If  $U > U_{min}$ , a glow discharge is initiated between the cathode and the grid. => electrons from the glow discharge plasma can migrate rapidly through the openings in the grid to the main discharge region between the grid and the anode. => thyatron closes.
- Operating voltage: several times 10 kV. After ignition:  $\sim 100 \text{ V}$  => an appreciable power loss occurs and need to be dealt with by cooling.
- Delay:  $\sim 200 \text{ ns}$ ; jitter:  $\sim \text{ns}$
- To regain the initial hold-off voltage: anode voltage must become slightly negative for 25-75  $\mu\text{s}$  for plasma to decay.

- A thermionic cathode is used in a thyatron.
  - Advantage: absence of a marked cathode potential drop using hot cathode.
  - If cold cathode is used, potential drop is needed to accelerate the ions for secondary-electron production => lead to erosion of the cathode and thus the lifetime.
  - A baffle is used as a screening element to avoid electron directly reaching the anode and causing the damage. It is shifted relatively to the grid to prevent a direct line of sight between cathode and anode.
- Operating times:  $10^5$  hours; Repetition rates: few kHz; Operating power: MW.

§4.1.1.7 The pseudospark switch





- The pseudospark switch operates in a low-pressure regime, where the mean free path of electrons and ions become comparable to the electrode spacing. Most electrons reach the anode without any ionizing collisions in the gas.
- Hollow cathode: increases the possible discharge path lengths.
- The diameter of the aperture determines the field penetration into the hollow cathode.
- A small number of initial electrons, triggered discharge in the hollow cathode for example, can initiate the pseudospark discharge.
- The switching mechanism is based on the build-up of a highly ionized plasma.
  - plasma build-up occurs first inside the hollow cathode where  $E/P$  is low.
  - Ions drift back into the hollow cathode  $\Rightarrow$  forming a positive space charge (virtual anode)
  - Static electric field inside the hollow cathode is distorted.
  - Electron production rate  $>$  loss rate in the hollow cathode and subsequently in the anode-cathode gap.
  - A low-resistivity plasma is established, and breakdown of the gap occurs.
- Jitter: 10 ns; Delay: 0.5  $\mu$ s.

#### §4.1.1.8 Ignitrons

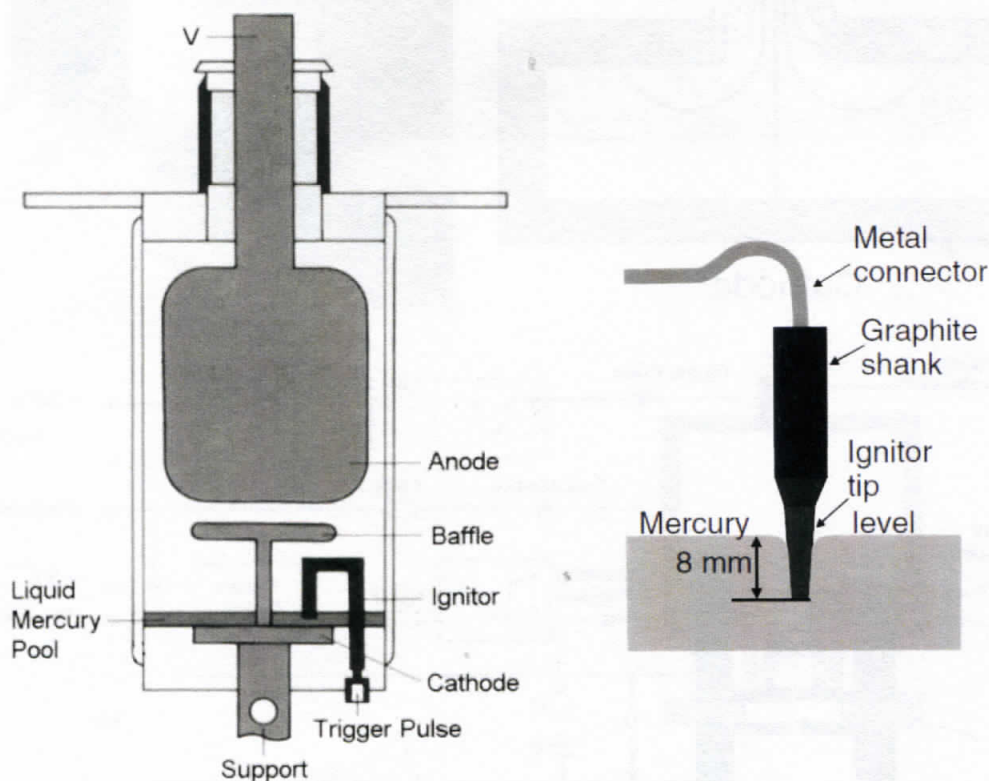


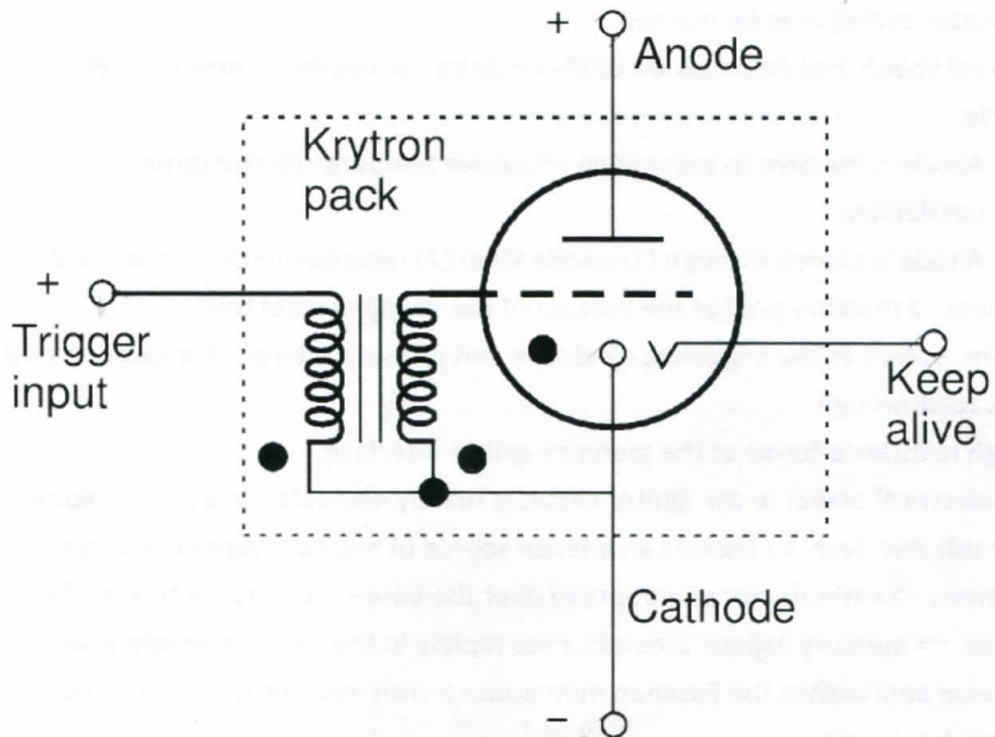
**Fig. 4.19.** High-voltage ignitron with splash baffle, and with a schematic illustration of the ignitor pin set-up. An enlarged view of the mercury contact to the trigger pin is shown on the *right*

- Ignitron is a very high-current, high-voltage switch with
  - a liquid mercury pool cathode
  - an ignitor pin dipping into the liquid-metal reservoir.
- Internal mercury pressure: ~5 Pa
- Can switch a pulse charge of up to 2000 Colum.
- Air/water cooled may be needed.
- Internal splash and deionization baffles may be contained in some devices.
- Anode:
  - Anode is massive to prevent an impulsive temperature rise during conduction.
  - Anode is cooled through (1) anode stem (2) radiation to the cooled walls.
- Cathode: a mercury pool at the bottom of the stainless steel tube.
- Ignitor: serves as the triggering electrode and is insulated from the cathode by a glass feedthrough.
- A high resistance forms at the mercury-ignitor interface.
- The electrical power in the ignitor circuit is mainly dissipated in a small volume near this interface. => creates an intense source of mercury vapour and free electrons => cathode hot spots spread over the entire mercury surface in ~50-100 ns. => mercury vapour pressure rises rapidly in the cathode-anode space. => pd value approaches the Paschen minimum => with free electrons, ionization avalanche develops.
- Rise time ~ 300-500 ns.
- After current drops below a critical value => no more additional vapour is produced => with additional time to allow recombination and recondensation of mercury.
- The mercury vapour must be forced to recondense back into the pool.
- Repetition rate ~1 Hz
- Progressively eliminated due to the mercury-containing waste.

§4.1.1.9 Krytrons

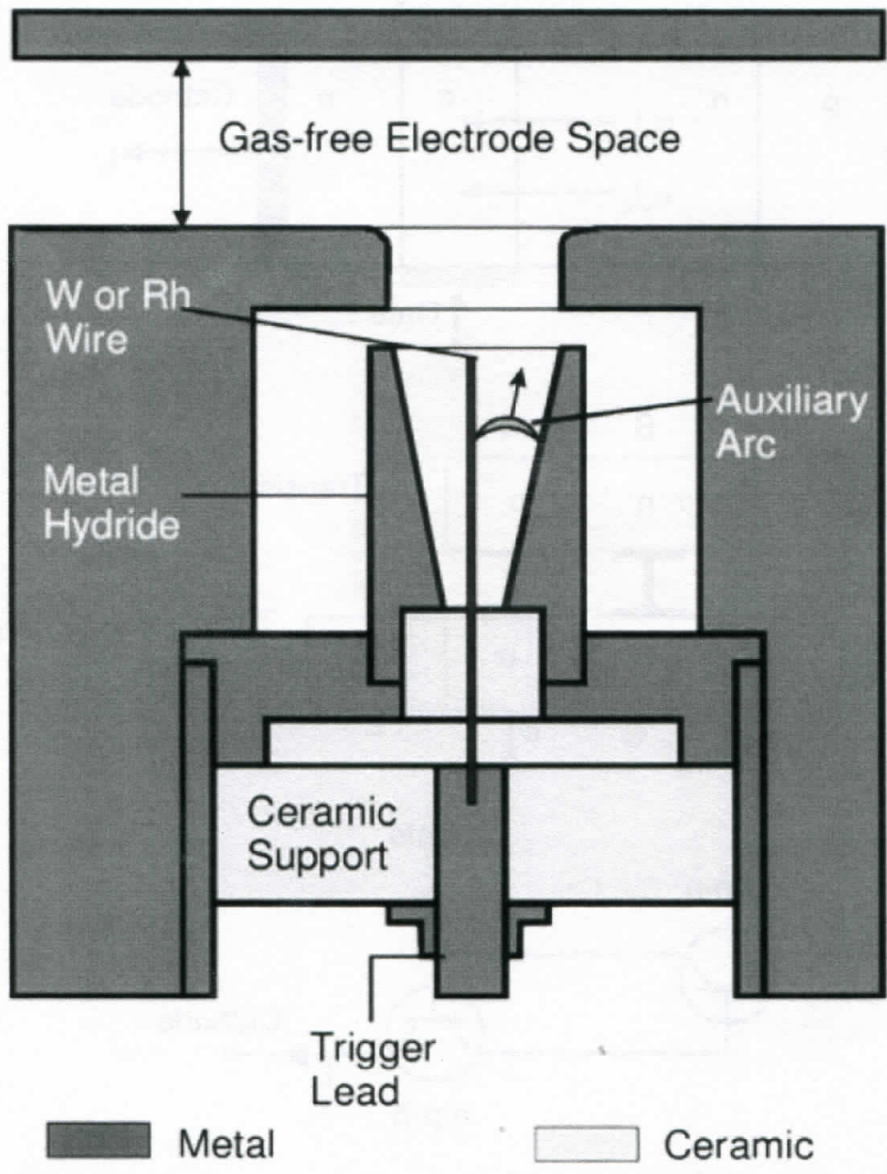
- Low-pressure gas discharge device with a tetrode configuration, sealed in a glass tube with a cold cathode.
- 1.3 kPa of helium gas.
- A special design of the anode-grid area + applied gas pressure -> large hold-off voltage.
- An already existing plasma is created by a glow discharge between the special keep-alive electrode and the cathode. => short trigger delay: ~30 ns.
- Rise time: ~1 ns,  $V_{max}$ : 8kV,  $I_{max}$ : 3 kA.

- Pulse length ~10  $\mu$ s, repetition rate ~1 kHz
- A positive pulse at the control grid initiates the switch.
- A  $^{63}\text{Ni}$   $\beta$ -emitter may be enclosed to create a weak permanent pre-ionization.
- It is widely used in fast trigger generators and Pockels cell driver and also ideal for use in the detonating circuitry of bombs.



#### §4.1.1.10 Triggered Vacuum Gap (TVG)

- A three-electrode system with  $P=0.001$  Pa.
- Closed by injection of a plasma cloud.
- Hold-off voltage depends on the properties of the electrode surfaces.
- I up to 10 kA, V up to 100 kV. Repetition rates of several kHz are possible if cooled.
- The gas-plasma mixture is created with the help of an auxiliary arc, burning between two electrodes inserted into one of the main electrodes.
- Jitter  $\sim 30$  ns; switching time  $\sim 100$  ns.



§4.1.2 Semiconductor closing switches

The limiting switching characteristics of semiconductor devices are:

- Relatively low mobility
- Low density of charge carries
- Comparatively low operating temperature

=> Large volume of the conducting region is required to conduct large currents.

§4.1.2.1 Thyristors

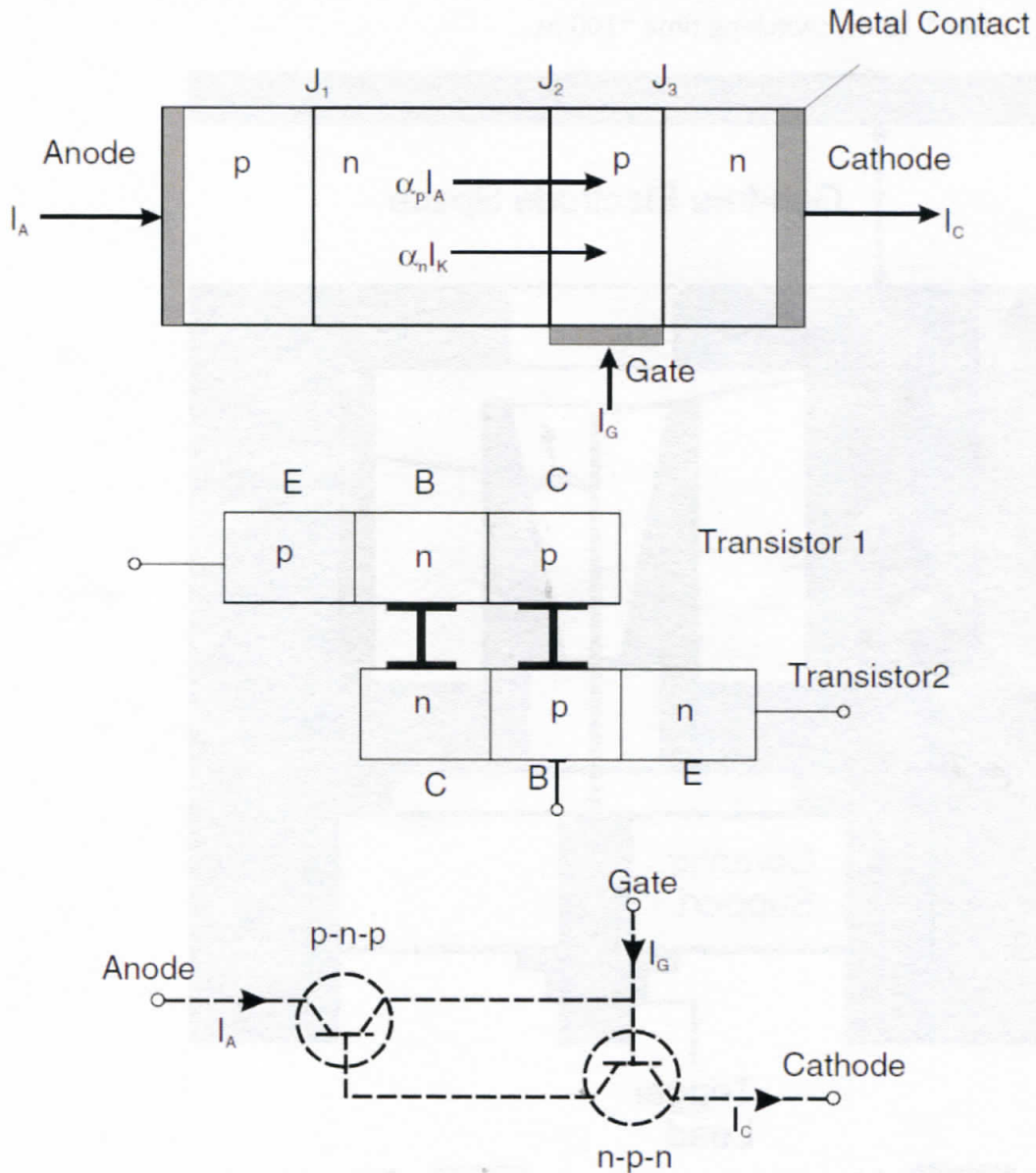
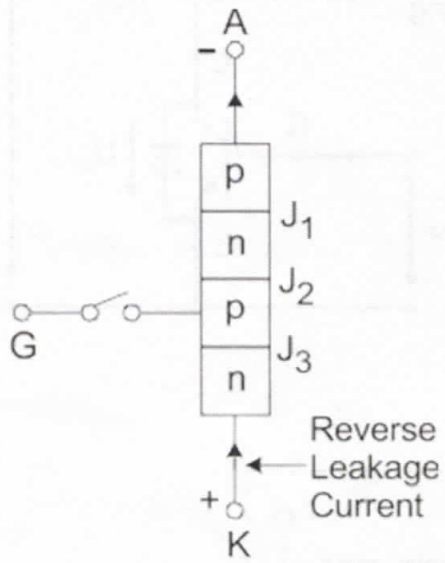
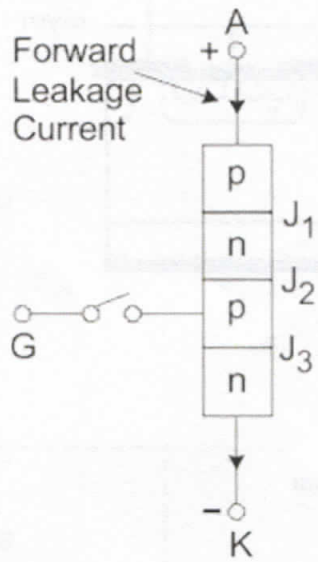


Fig. 4.22. Structure of thyristor, and two-transistor equivalent circuit

- Three modes of operation:
  - Reverse blocking state
  - Forward blocking state
  - Conduction or on state



Reverse Blocking Mode



Forward Biased Condition

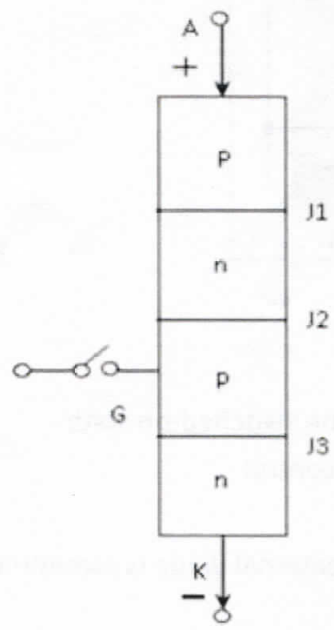


Fig 1: Forward blocking

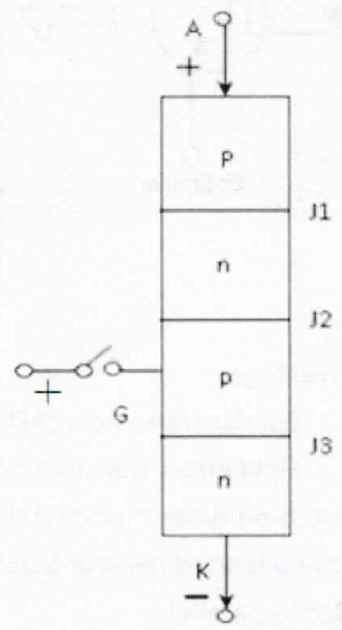
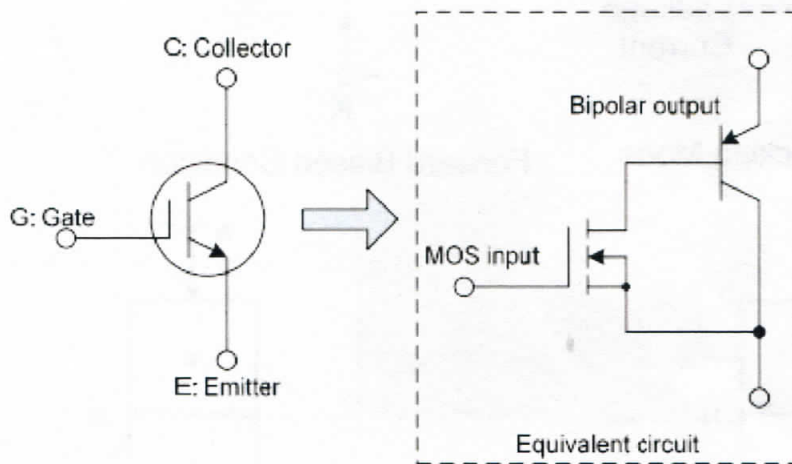
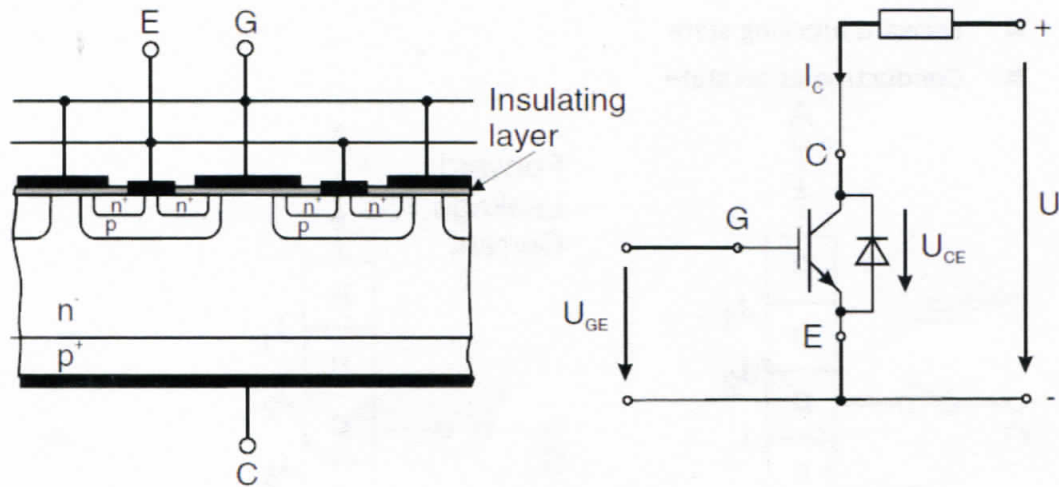


Fig 2: Forward Conduction

§4.1.2.2 IGBTs



- Advantage:
  - Bipolar transistors (BJT) – low resistance in the switched-on state
  - Field effect transistors (FET) – loss-free gate control
- Switch-on times ~ several times 10 ns.
- It has a limited reverse-blocking capability => an external diode is sometimes used in parallel.
- High-power IGBT: blocking voltages  $V \sim 4$  kV, on state  $I \sim 3$  kA

§4.1.2.3 Optically activated semiconductor switches

$$\nabla j_n = e(R_n - G_n) + e \frac{\partial n}{\partial t}$$

$$\nabla j_p = -e(R_p - G_p) - e \frac{\partial p}{\partial t}$$

$$eG_{av} = \alpha_n |j_n| + \alpha_p |j_p|$$

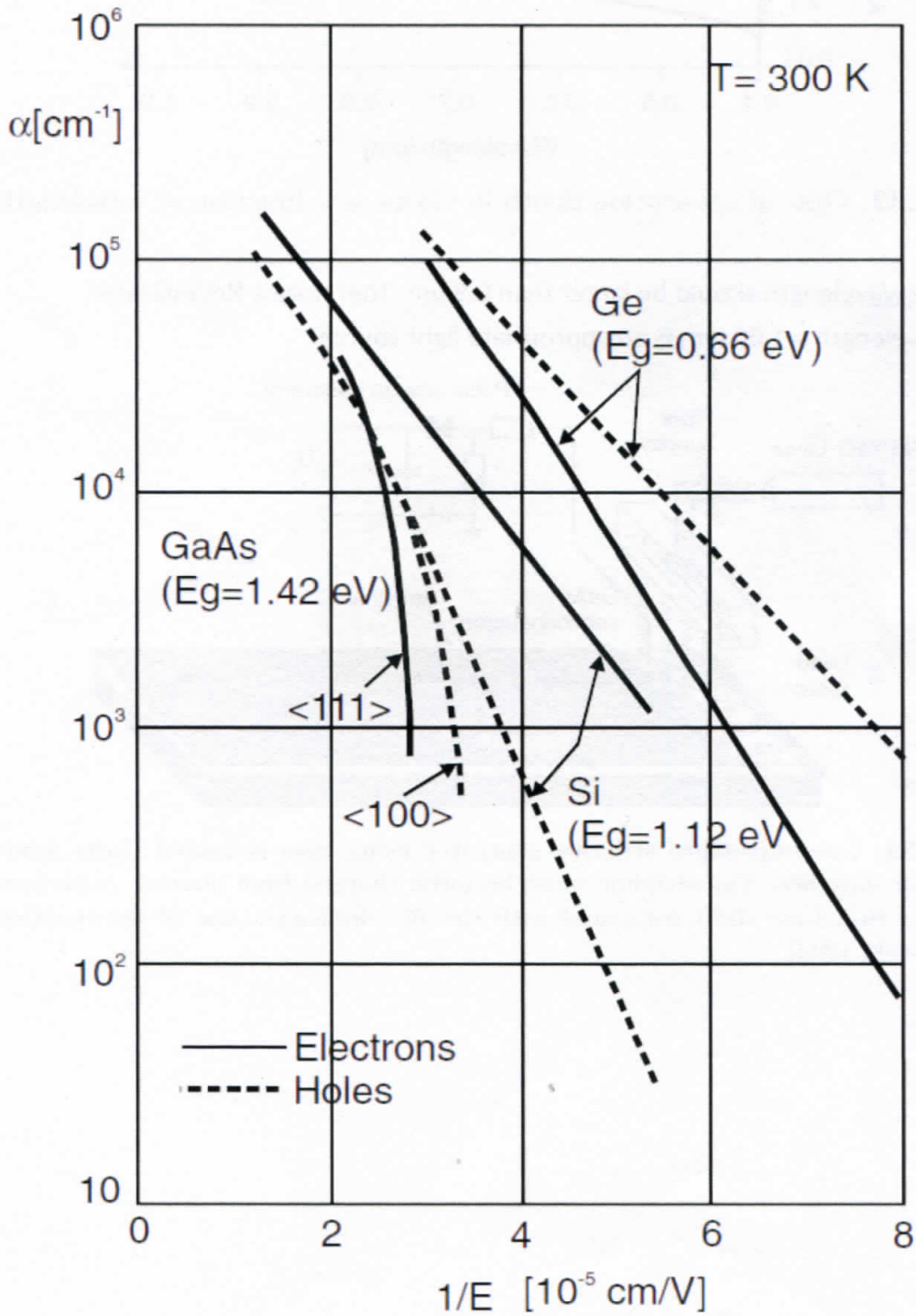


Fig. 4.31. Ionisation rate coefficients  $\alpha_n$  and  $\alpha_p$



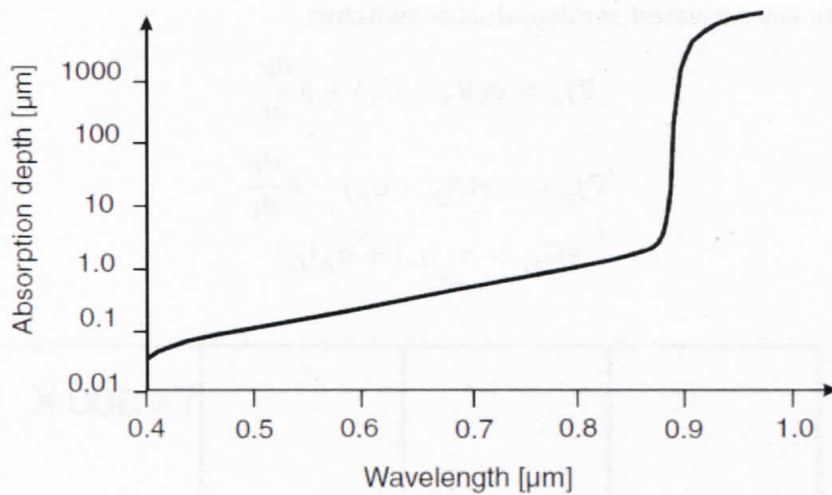


Fig. 4.32. Optical absorption depth in GaAs as a function of wavelength

- The wavelength should be larger than 0.9 μm. Therefore a Nd:YAG laser, wavelength = 1.06 μm, is an appropriate light source.

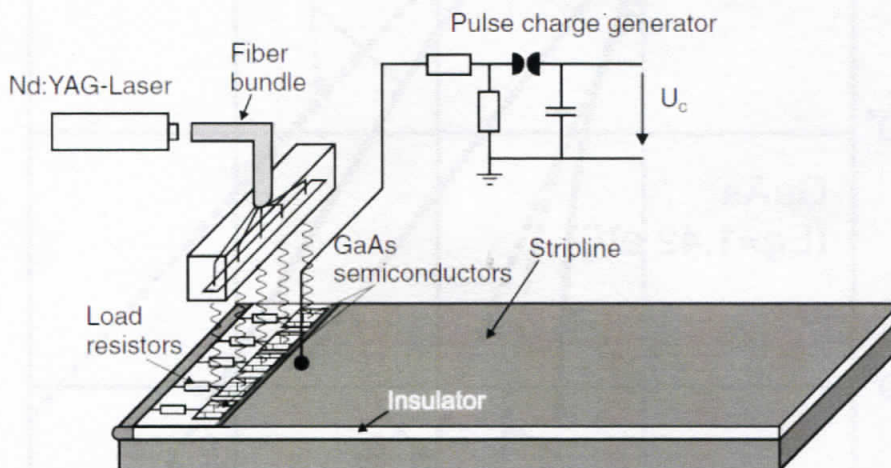
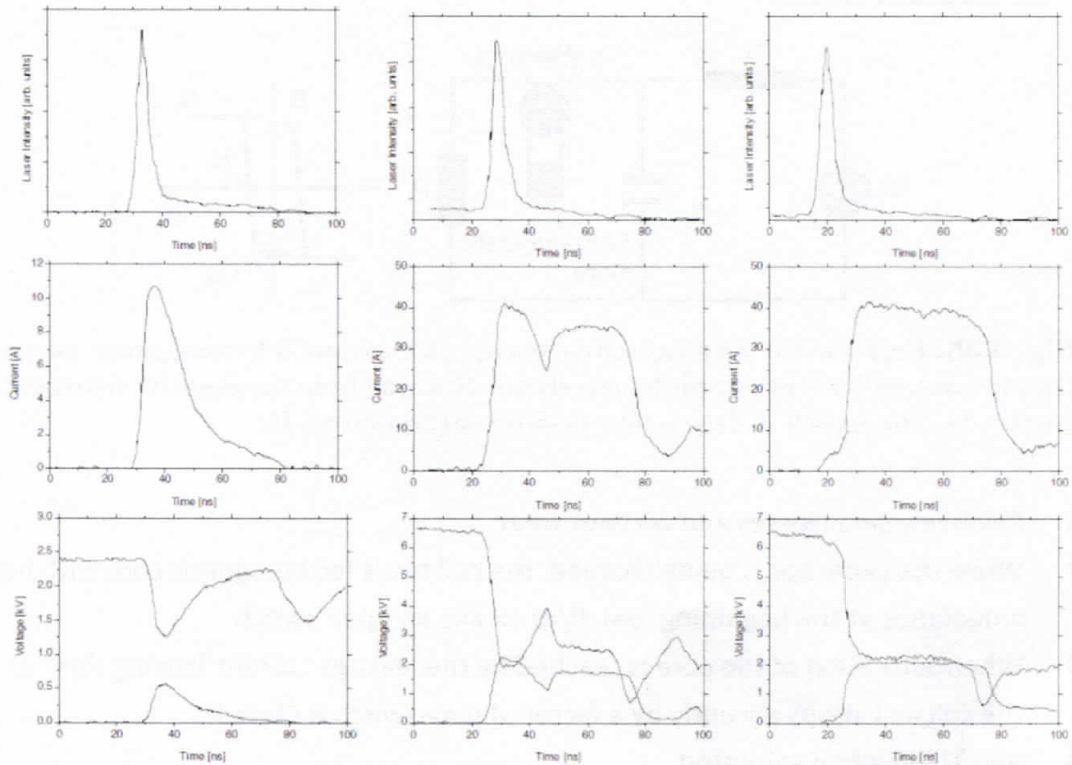


Fig. 4.33. Low-impedance stripline generator using laser-activated GaAs semiconductor switches. The stripline must be pulse charged from another capacitive generator in a time short compared with the  $RC$  discharge time of the stripline [Katschinski 1994]



**Fig. 4.34.** A collection of signals measured with the set-up of Fig. 4.33. The stripline was charged to 2.4kV (*left*) and 6.4kV (*middle* and *right*). The left compilation demonstrates the typical performance in the linear photoconducting regime of operation, while the right sequence refers to the nonlinear avalanche regime. The diagrams in the central part of the figure show the transition between the two regimes. In the *bottom* row the voltage across the switch and across a load resistor are shown [Katschinski 1994]

- Linear photoconducting regime: the available number of charge carriers is determined only by the laser intensity
- Nonlinear regime: the number of charge carriers is increased by collisional ionization and as in a gas switch increases exponentially.

§4.1.3 Magnetic Switches

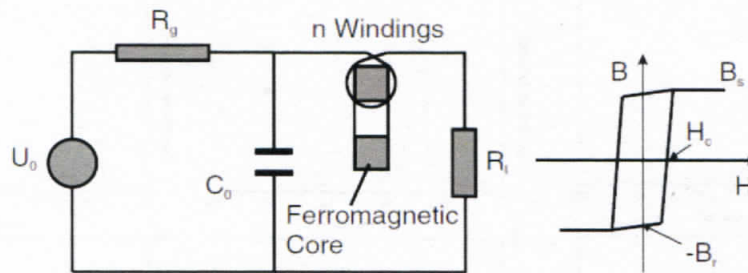


Fig. 4.35. Basic circuit with capacitive energy storage and a ferromagnetic switch. On the right, an ideal hysteresis loop is shown. Starting from the negative remanence point  $-B_s$ , the switch is driven into positive saturation at  $B_s$ .

- Relatively small losses and without wear
- While the capacitor is being charged: the coil has a ferromagnetic core with high inductance at the beginning:  $V=Ldi/dt \Rightarrow$  like an open switch
- When saturation of the core is reached by the leakage current flowing through the coil  $\Rightarrow L$  drops abruptly by a factor of  $\mu \Rightarrow$  switch is closed.
- $\mu=B/H \rightarrow 0$  when saturated
- The hysteresis loop should approximate a rectangular form, with an abrupt change of the permeability over several orders of magnitude when the saturation point is reached.

## §4.1.4 Summary

**Table 4.2.** Summary of properties of closing switch

Type	Hold-off potential (kV)	Peak current (kA)	Cumulative charge (A s)	Repetition rate (Hz) [commutation time (ns)]	Lifetime (number of pulses)	Remarks
Spark gap	1-6000	$10^{-3}$ -1000	0.1-50	1-10 [1-1000]	$10^3$ - $10^7$	Lifetime is determined by electrode erosion
Thyratron	5-50	0.1-10	$10^{-3}$	1000 [5-100]	$10^7$ - $10^8$	Applied in lasers and accelerators
Ignitron	> 10	> 100	2000	1 [1000]	$10^5$ - $10^6$	Applied in lasers and accelerators
TVG	0.5-50	1-10	40	1 [10-100]	$> 10^4$	
Pseudo-spark	1-50	1-20	1	1-1000 [ $> 10$ ]	$10^6$ - $10^8$	Similar to Thyratron
Krytron	8	3	0.01-0.1	$< 1000$ [1-10]	$10^7$	Very short delay and commutation time
Magnetic Switch	1000	100-1000		10 [5-10000]	$10^8$ - $10^9$	Cannot be triggered; one operating point only
Thyristor	$< 5$	$< 5$	$10^{-2}$	10 [ $> 1000$ ]	$10^8$	Can be stacked; expensive; complex
IGBT	$< 4$	3		100	$10^8$	Can be switched off
GaAs photoactivated switch	$< 20$	1-10	$< 10^{-4}$	$< 10$ [1-10]	$10^2$ - $10^3$	Needs intense light source

## 7 4.2 Opening Switches.

\* An opening switch is characterised by

"a sudden growth of its impedance." by

- external actuator

- internal process  $\rightarrow$  depend on the amount of the charge conducted through the switch.

\* The mechanism can be:

- resistive  $\rightarrow$  common fuse

- inductive  $\rightarrow$  nature  $\rightarrow$  flux compression,  $L(t) > L_0$

- capacitive  $\rightarrow C(t) < C(0)$

\* Examples:  $\rightarrow$  common fuse

$\rightarrow$  etc

\* Fr

\* Requirement:

- Long current conduction time.

- Large current & small ~~current~~ losses during conduction.

- ~~Fast~~ Fast impedance rise during opening.

- high impedance after opening & large voltage hold-off during current interruption.

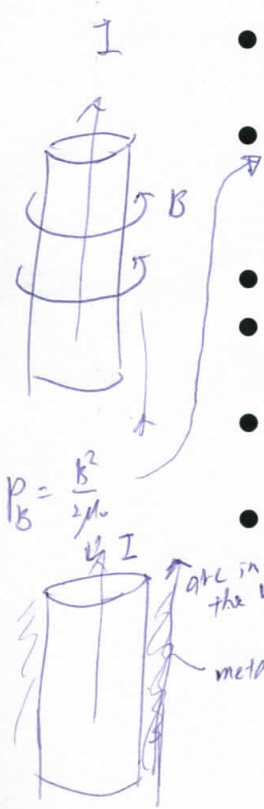
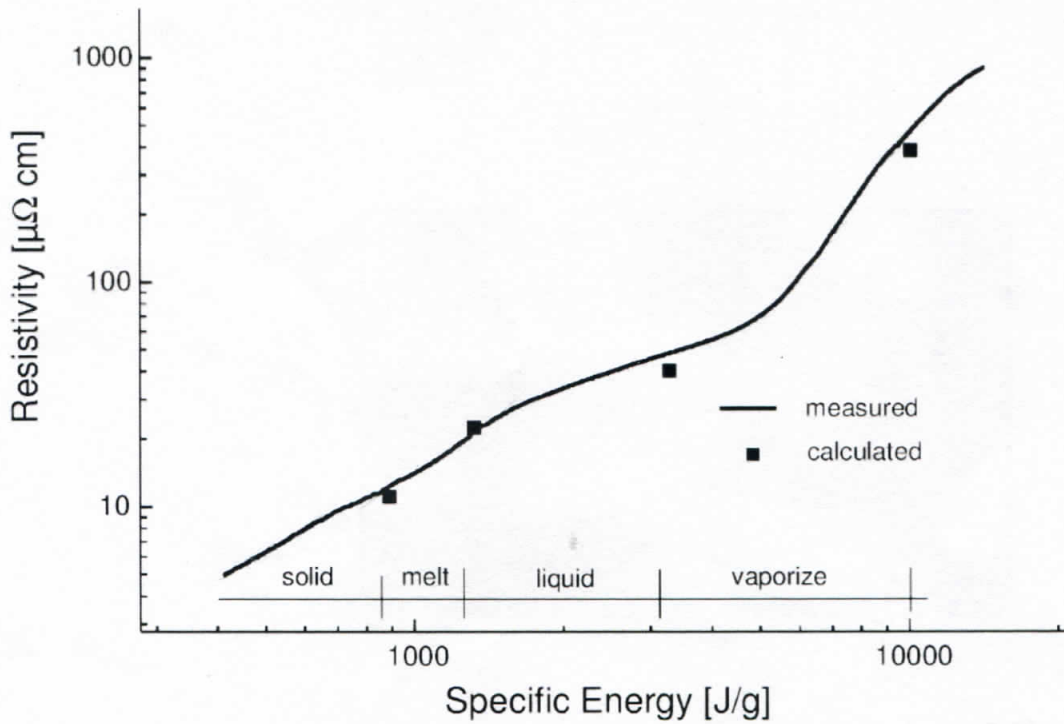
- Short recovery time (i.e. high repetition rate capability)

- Long lifetime (small wear).

7 7f

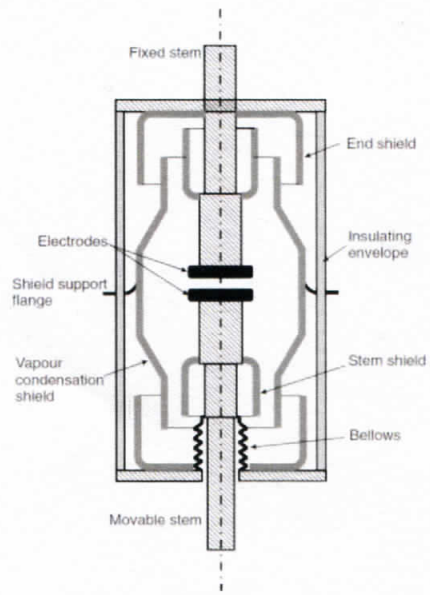
### §4.2.1 Fuses

- Melting fuse – the most widely known opening switch
  - A thin wire / a foil embedded in a gaseous, liquid or granular medium
- Based on **Melting, Boiling, or Vaporization** of a conductor
- Fast opening is possible - <50 ns
- Conduction time can be determined by the type of material and its geometry

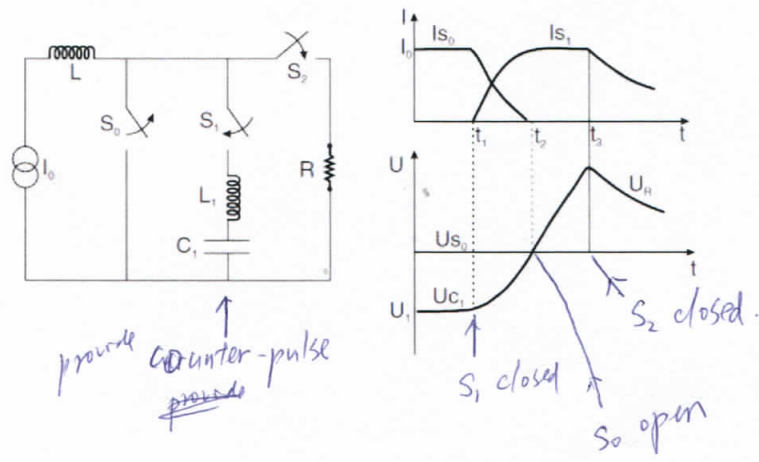


- The resistivity of most metals rises continuously with  $T$  both in the solid and in the liquid phase.
- The high magnetic pressure associated with the current flowing through the fuse can maintain a high density and therefore metallic conductivity beyond the critical temperature.
- Only after the onset of expansion does the metallic conductivity disappear.
- If the density of the metal vapor becomes sufficiently small  $\rightarrow$  electron avalanche processes can lead to the initiation of arcs in the vapor.
- The purpose of the **surrounding medium** is therefore to **quench** or **prevent** arc formation.
- Advantage – **simplicity, adapt** their parameters to the experimental conditions by choosing the appropriate **cross-section, length, and #/ of elements**.

### §4.2.2 Mechanical Interrupters



- Vacuum interrupter switch: 2 planar/disc electrodes (1 fixed the other movable) in a vacuum envelope (0.1 Pa or less).
- Closed position – low resistance (10-50 uOhm) from a tight metal-to-metal contact
- Open position – separated by an actuator (致動器).
- During the process of switch breaking – an **arc** is likely to be drawn and sustained by **metal vapor** evaporated from the electrodes.
- In unipolar system, a **current counter-pulse** is needed to reduce the power input to the arc to allow the residual arc plasma to recombine.
- After  $I=0$ ,  $dU/dt=24 \text{ kV/us}$  is possible.
- Repetitive frequency – few tens of hertz.
- Opening speed – tens of us.



### §4.2.3 Superconducting opening switches

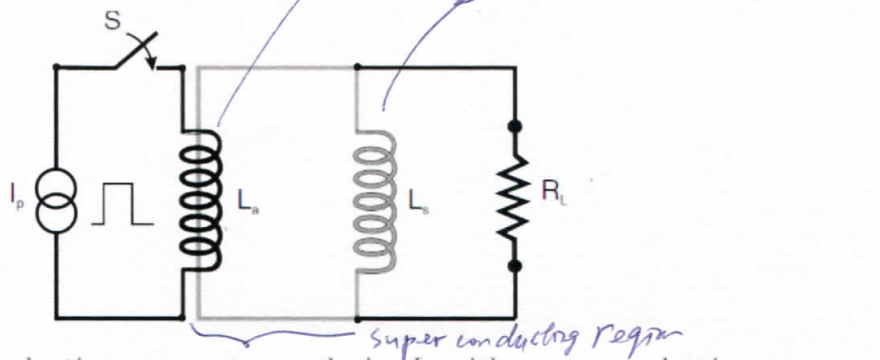
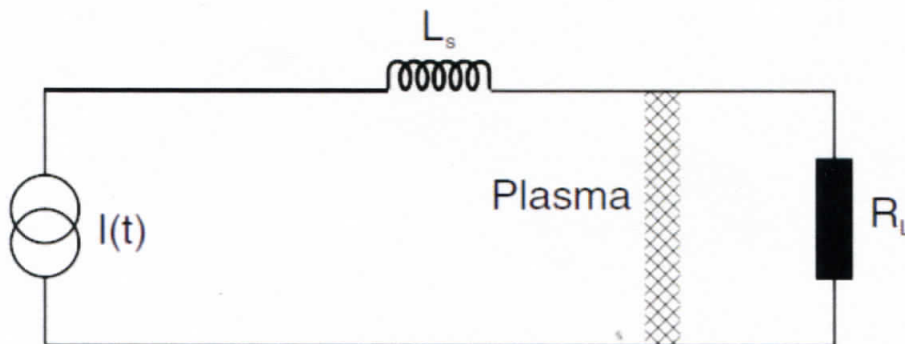


Fig. 4.40. Superconducting energy storage device  $L_s$  with a superconducting opening switch activated by a pulsed-magnetic field coil  $L_a$ , which creates a field above the critical value in a section of the superconducting circuit. The resistance of this section must become larger than the load resistance  $R_L$  to divert the current into the load effectively

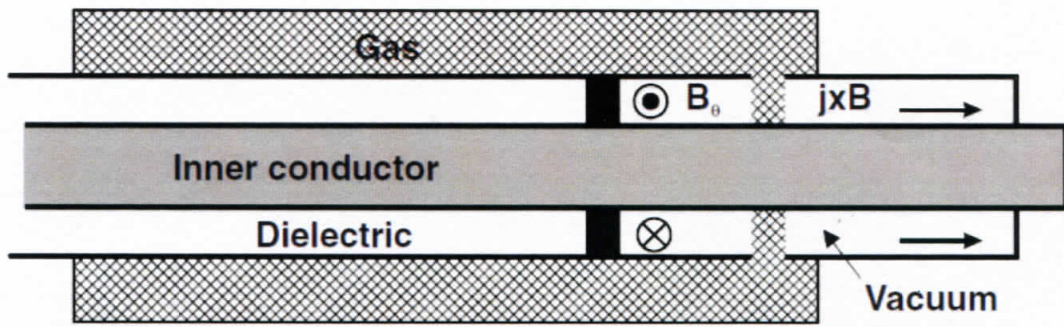
- Superconducting state -> normal conduction
- Problem: consists of the additional cooling necessary to remove the heat flowing into the cryogenic coolant during opening.
- Three ways to trigger
  - the current itself
  - an external pulsed magnetic field
  - pulse heating
- The repetition rate depends on the **speed of recovery to the superconducting state.**

### §4.2.4 Plasma opening switches

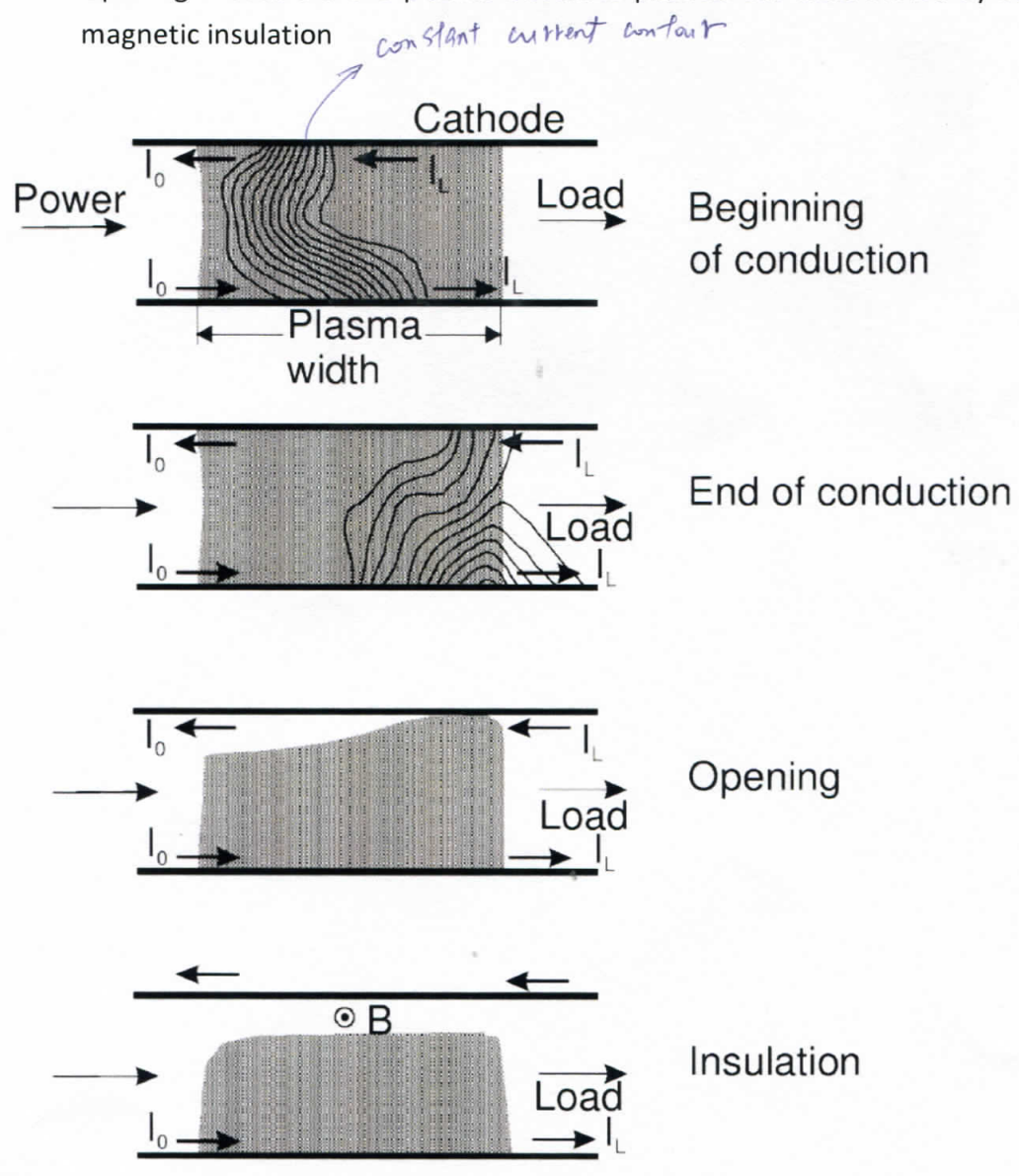


- Suitable for high currents and short switching times
- Plasma bridge of low density ( $10^{13}$ - $10^{15}$   $\text{cm}^{-3}$ )
  - $10^{15}$ - $10^{16}$   $\text{cm}^{-3}$  for several hundred kA or MA
  - $10^{13}$   $\text{cm}^{-3}$  is needed to conduct currents for less than 100 ns and opening in less than 10 ns.



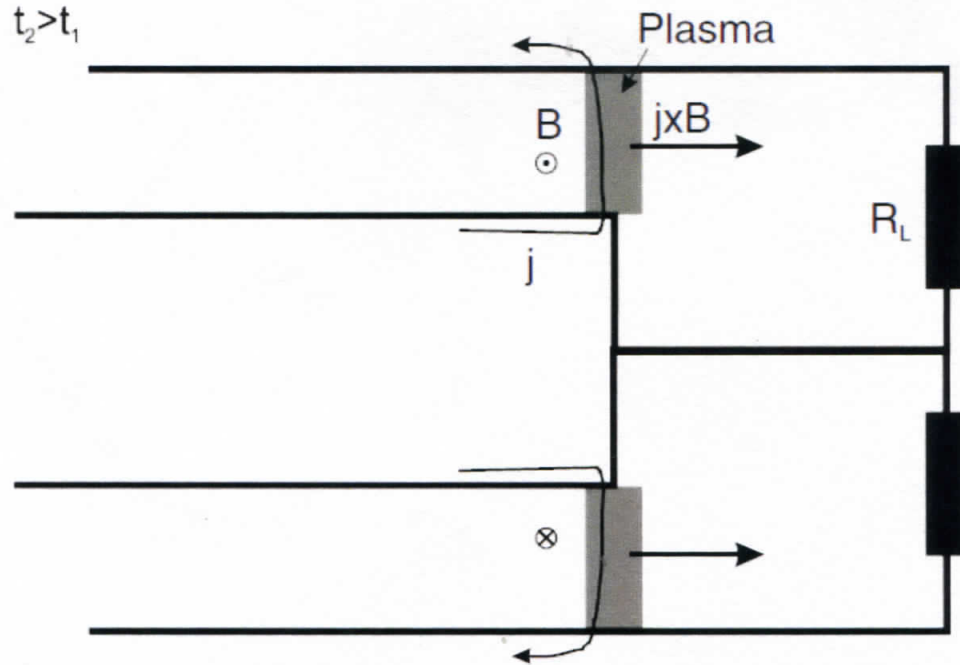
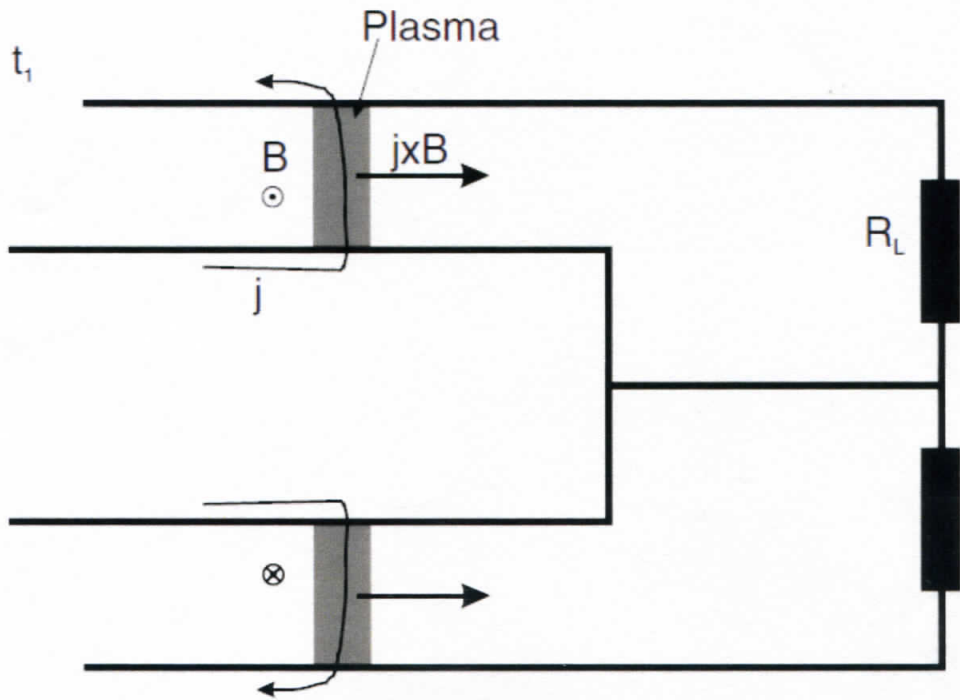


- A coaxial system is shown above where the gas is made into a plasma by an auxiliary electric pulse before the coaxial inductor is charged.
- Conduction phase – the current, the magnetic field penetrates into the plasma
- Opening – occurs if the plasma becomes pushed out determined by self-magnetic insulation



### §4.2.5 Plasma Flow Switches

- Higher plasma densities ( $10^{15} \text{ cm}^{-3}$ )
- Conduction times – us



## \$5 Pulse-Forming Networks

- A constant-voltage plateau is needed for many pulsed-power applications.
- Various arrangements of LC elements are necessary -> called Pulse-Forming Networks.

### \$5.1 Transmission Lines

- Transmission lines are the continuous borderline case of a network consisting of discrete LC elements.
- Lumped circuit element? Or an extended object? -> depends on the time T during which energy is extracted from or supplied to the element:
  - $T >$  the time it takes for an EM wave to move from one terminal of the element to the next -> lumped circuit element.
  - $T <$  the time it takes for an EM wave to move from one terminal of the element to the next -> Transmission line.
- Different kinds of transmission line and the inductance and the capacitance per unit length is given in the following:

Table 5.1. Transmission line geometries and distributed parameters

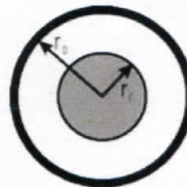
1. Coaxial transmission line:

$$C' = 2\pi\epsilon / \ln(r_o/r_i)$$

$$L' = (\mu/2\pi) \ln(r_o/r_i)$$

$$Z_0 = \left( (\mu/\epsilon)^{1/2} / 2\pi \right) \ln(r_o/r_i)$$

$$= 60(\mu_r/\epsilon_r)^{1/2} \ln(r_o/r_i)$$

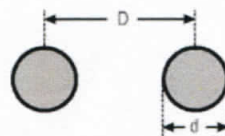


2. Double-wire line:

$$C' = \pi\epsilon / \operatorname{arcosh}(D/d)$$

$$L' = (\mu/\pi) \operatorname{arcosh}(D/d)$$

$$Z_0 = \left( (\mu/\epsilon)^{1/2} / \pi \right) \operatorname{arcosh}(D/d)$$

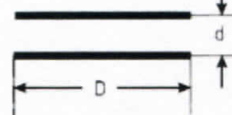


3. Parallel-plate line:

$$C' = \epsilon D/d$$

$$L' = \mu d/D$$

$$Z_0 = (\mu/\epsilon)^{1/2} (d/D)$$

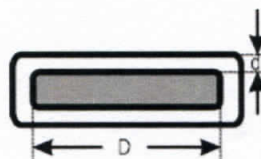


4. Stripline:

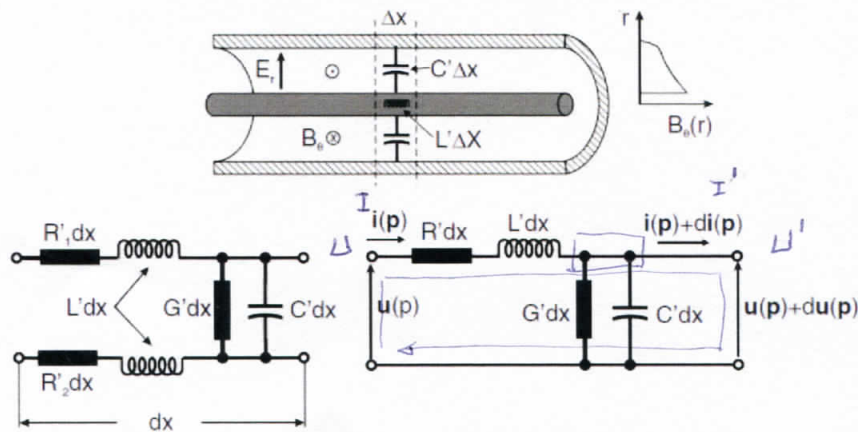
$$C' = 2\epsilon D/d$$

$$L' = \mu d/2D$$

$$Z_0 = (\mu/\epsilon)^{1/2} (d/2D)$$



- An infinitesimal section of a homogeneous coaxial transmission line:



- Resistances per unit length:  $R_1 + R_2 \rightarrow R$
- Conductance per unit length:  $G$
- All quantities are frequency-dependent because of the skin effect and because the dielectric constant depends on the frequency.
- Assume: they are independent of the position  $x$  and the voltage  $V$  and current  $I$  as well.

$$\rightarrow \begin{aligned} U - IR dx - L dx \frac{dI}{dt} - U' &= 0 \Rightarrow \frac{U' - U}{dx} = \frac{\partial U}{\partial x} = -RI - LI \\ \dot{I} - U' G dx - \underbrace{C dx}_{Q=Cv} \dot{U}' - I' &= 0 \Rightarrow \frac{I' - I}{dx} = \frac{\partial I}{\partial x} = -GU' - CU' \\ I &= \frac{v}{R} = GV \quad Q = Cv \quad I = \dot{Q} = c\dot{v} \end{aligned}$$

Laplace transform  $\chi = \tilde{\chi} e^{pt} \Rightarrow \frac{d}{dt} \rightarrow p$

$$\Rightarrow \begin{cases} \frac{d\tilde{U}}{dx} = -R\tilde{I} - pL\tilde{I} = -(R+pL)\tilde{I} \\ \frac{d\tilde{I}}{dx} = -G\tilde{U} - pC\tilde{U} = -(G+pC)\tilde{U} \\ \frac{d^2\tilde{U}}{dx^2} = -(R+pL)\frac{d\tilde{I}}{dx} = (R+pL)(G+pC)\tilde{U} \\ \frac{d^2\tilde{I}}{dx^2} = (G+pC)\frac{d\tilde{U}}{dx} = -(G+pC)(R+pL)\tilde{I} \end{cases}$$

\* Lossless line where  $R=0, G=0$ .

$$\begin{cases} \frac{d^2 \tilde{U}}{dx^2} = p^2 C \cdot L \tilde{U} \\ \frac{d^2 \tilde{I}}{dx^2} = p^2 C \cdot L \tilde{I} \end{cases}$$

$$\Rightarrow U(x, p) = U_x(p) = \begin{cases} \tilde{U}_+ e^{-p\sqrt{LC}x} \\ \tilde{U}_- e^{p\sqrt{LC}x} \end{cases}$$

Inverse Laplace transform:

$$\mathcal{L}\{U_x(t-\tau)\} = \tilde{U}_+ e^{-p\tau} \quad \text{function}$$

$$\Rightarrow U(x, t) = U_x(t) \begin{cases} U_+(t-x\sqrt{LC}) \\ U_-(t+x\sqrt{LC}) \end{cases}$$

or Linear combination:

$$U_x(t) = U_+(t - \frac{x}{c}) + U_-(t + \frac{x}{c})$$

where  $c \equiv \frac{1}{\sqrt{LC}}$

$$\frac{d\tilde{U}}{dx} = -p \cdot L \tilde{I}$$

$$+p\sqrt{LC} \tilde{U}_+ = +pL \tilde{I}_+$$

$$\frac{\tilde{U}_+}{\tilde{I}_+} = \sqrt{\frac{L}{C}} \equiv Z_0 = -\frac{\tilde{U}_-}{\tilde{I}_-}$$

For loss-free transmission line,

$$Z_0 = \frac{U_+(t-x/c)}{I_-(t-x/c)} = -\frac{U_-(t+x/c)}{I_-(t-x/c)}$$

# 7.5.1.1 Terminations & Junctions p109

- lossless transmission line terminates with an arbitrary freq-dependent impedance  $Z(p)$   
In Laplace space

$\Omega$ 's Law:  $Z(p) = \frac{\hat{U}_+ + \hat{U}_-}{\hat{I}_+ + \hat{I}_-}$

$\therefore \hat{U}_+ = Z \hat{I}_+ \quad , \quad \hat{U}_- = -Z_0 \hat{I}_-$

$\Rightarrow Z = \frac{\hat{U}_+ + \hat{U}_-}{\hat{I}_+ - \frac{\hat{U}_-}{Z_0}} = Z_0 \frac{1 + \hat{U}_-/\hat{U}_+}{1 - \hat{U}_-/\hat{U}_+} = Z_0 \frac{1 + \rho}{1 - \rho}$

$\rho = \frac{\hat{U}_-}{\hat{U}_+}$  is the reflection coefficient

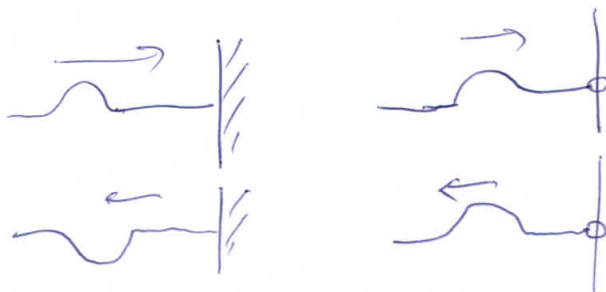
$\Rightarrow Z - Z_0 = (Z + Z_0)\rho \Rightarrow Z - Z_0 = (Z + Z_0)\rho$

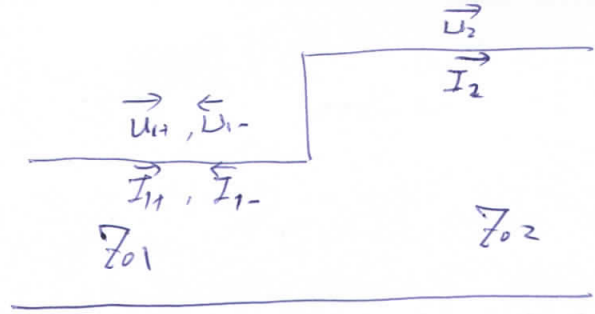
$\rho = \frac{\hat{U}_-}{\hat{U}_+} = \frac{Z - Z_0}{Z + Z_0}$

$\Rightarrow$  Match Load:  $Z = Z_0$  ,  $\rho = 0$

Short-circuit case:  $Z = 0$  ,  $\rho = -1 \rightarrow$  Completely reflection with inverted voltage amplitude

Open-circuit case:  $Z = \infty$  ,  $\rho = 1 \rightarrow$  --- same polarity





$$\rho = \frac{U_{1-}}{U_{1+}} = \frac{Z_{02} - Z_{01}}{Z_{02} + Z_{01}}$$

$$U_{1+} + U_{1-} = U_{2+} \Rightarrow T \equiv \frac{U_{2+}}{U_{1+}} = 1 + \frac{U_{1-}}{U_{1+}} = 1 + \rho \quad \text{Transmission}$$

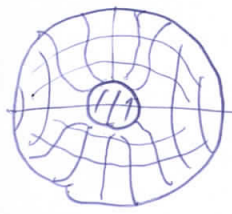
\* For  $Z_{01} = Z_{02}$  :  $\rho = 0$  ,  $T = 1$

$\Rightarrow$  Reflection-free junction  $\Rightarrow Z_{01} = Z_{02}$  is necessary but not sufficient  $\therefore$

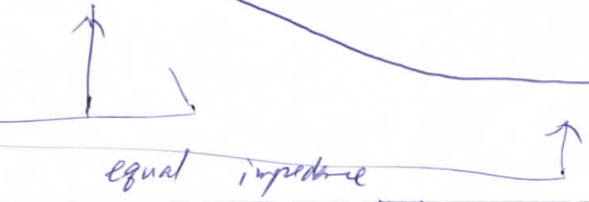
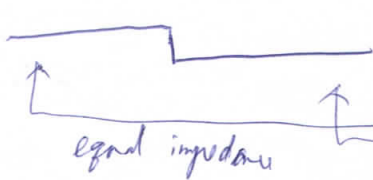
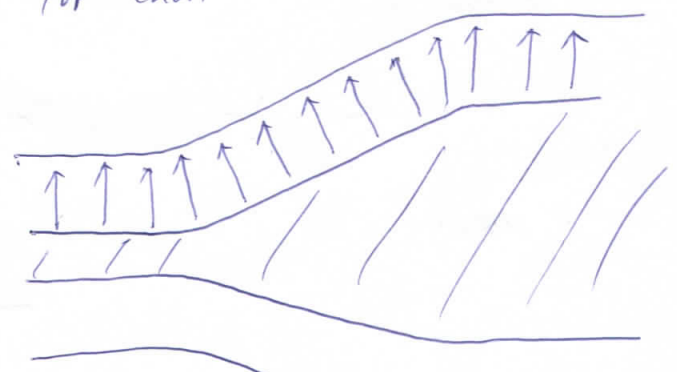
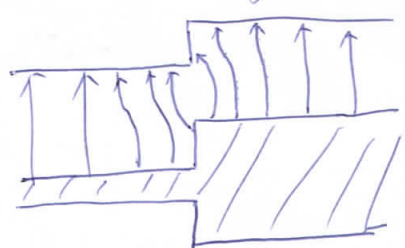
\* If the geometry of a line changes abruptly, it becomes impossible to satisfy Maxwell's eq. just by superposing the fundamental waves.

\* Only by a smooth transition can we achieve the condition that the fields are not disturbed too much & that the reflections can be avoided for high freq.

$\vec{E} \perp \vec{k}$  may not corrct  $\Rightarrow V_{\phi}$  is freq-dependent.



$H_{11}$  ( $TE_{11}$ ) mode has the lowest cutoff freq.



# § 5-1.2 Transmission Lines with losses

- \* Finite  $R$  of the conductor
- non-zero conductance & the high-freq. properties of the dielectric medium.
- radio emission in the case of an open system.

$$\frac{d^2 \tilde{U}}{dx^2} = (G + pC)(R + pL) \tilde{U} = p^2 L C (1 + \frac{G}{pC})(1 + \frac{R}{pL}) \tilde{U}$$

$$= p^2 L' C' \tilde{U}, \quad \text{where } L' = L(1 + \frac{R}{pL})$$

$$C' = C(1 + \frac{G}{pC})$$

$$\Rightarrow Z_0 = \sqrt{\frac{L'}{C'}} = \sqrt{\frac{L}{C}} \cdot \sqrt{\frac{1 + R/pL}{1 + G/pC}}$$

$$\approx \sqrt{\frac{L}{C}} (1 + \frac{R}{2pL}) (1 - \frac{G}{2pC}) \approx \sqrt{\frac{L}{C}} (1 + \frac{R}{2pL} - \frac{G}{2pC} - \frac{RG}{4p^2 LC})$$

$$\approx \sqrt{\frac{L}{C}} \left[ 1 + \frac{R/L - G/C}{2p} \right]$$

for high freq.  $R \ll pL, G \ll pC$

$$\Rightarrow \frac{1}{C} \approx \sqrt{LC} \left[ 1 + \frac{R/L - G/C}{2p} \right]$$

$$\vec{U}_{tot} = \vec{U}_0 e^{-\alpha x} e^{-j\beta x}$$

$$\vec{U} = \vec{U}_0 e^{-\alpha x} e^{-j\beta x}$$



$$\tilde{U}_{L,t} = \tilde{U}_{0,t} e^{-p\sqrt{LC}x} = \tilde{U}_{0,t} e^{-p\sqrt{LC} \cdot \sqrt{(1+R/2pL)(1+G/2pC)}x} \quad p.112$$

$$\hat{U}_{0,t} e^{-p\sqrt{LC} \left(1 + \frac{R}{2pL} + \frac{G}{2pC}\right)x}$$

$$= \hat{U}_{0,t} e^{-p\sqrt{LC} \left(\frac{R}{2pL} + \frac{G}{2pC}\right)x} e^{-p\sqrt{LC}x}$$

$$= \tilde{U}_{0,t} e^{-\left(\frac{R}{2}\sqrt{\frac{C}{L}} + \frac{G}{2}\sqrt{\frac{L}{C}}\right)x} e^{-p\sqrt{LC}x} = \tilde{U}_{0,t} e^{-ax} e^{-p\sqrt{LC}x}$$

$$a = \frac{R}{2}\sqrt{\frac{C}{L}} + \frac{G}{2}\sqrt{\frac{L}{C}} = a_R + a_G$$

↳ neglected for freq.  $< 10^9$  Hz

Owing to the skin effect,  $a_R \propto \omega^{1/2}$

$$\left( R = \sqrt{\frac{\mu\omega^2 \rho_a}{2}} R_a + \sqrt{\frac{\mu\omega^2 \rho_i}{2}} R_i \right)$$

⇒  $a = k\sqrt{\omega}$

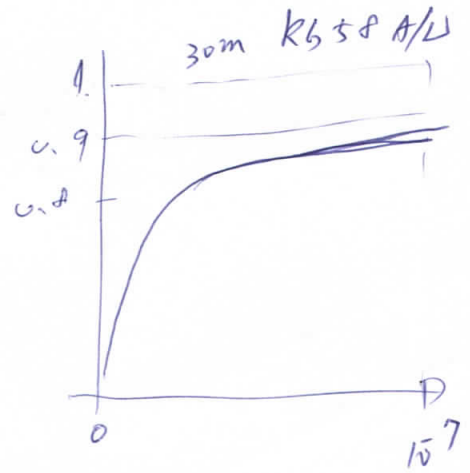
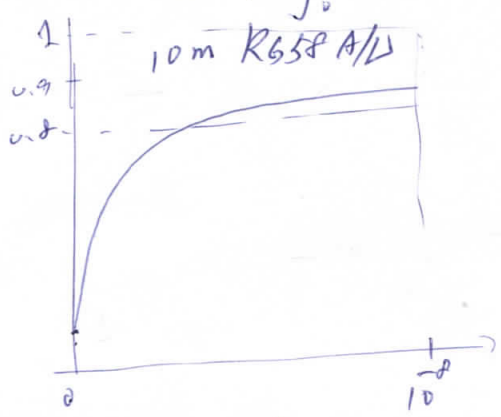


$$U(l,t) = U_0 \left[ 1 - \Phi\left(\frac{kx}{\sqrt{t-l/c}}\right) \right]$$

$$\Phi(s) = \frac{2}{\sqrt{\pi}} \int_0^s e^{-q^2} dq$$

← Gaussian error integral.

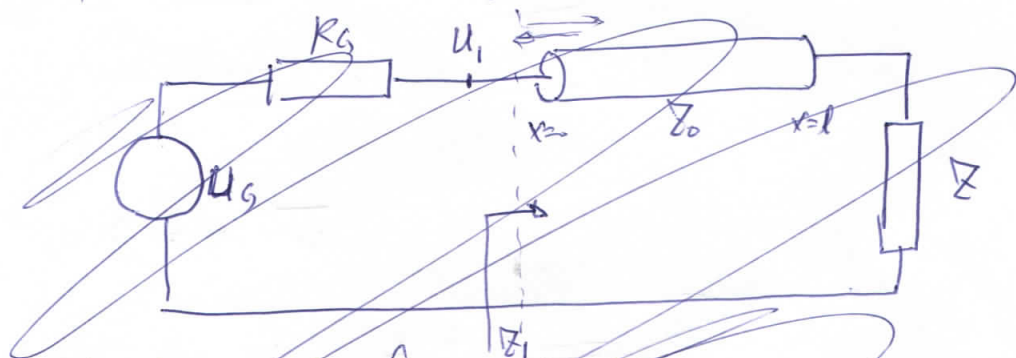
Relative amplitude



Time after arrival at cable exit (sec)

# §5.1.3 The finite Transmission line as a Circuit Element.

- \* Transmission line for its use as a circuit element:
  - the temporal delay that a signal experiences
  - its characteristic, resistor-like impedance
  - its signal reflection properties
- \* For slow signal or short cables, the input impedance of a cable w/ a non matched ~~termination~~ termination ( $Z \neq Z_0$ ), i.e. purely ohmic, but not complex:



Laplace transform: ← input impedance.

$$\hat{U}_i = \frac{Z}{R_G + Z} \hat{U}_G$$

$$\hat{U}_i = \hat{U}_{i+} + \hat{U}_{i-} = \hat{U}_{i+} \left( 1 + \frac{\hat{U}_{i-}}{\hat{U}_{i+}} \right)$$

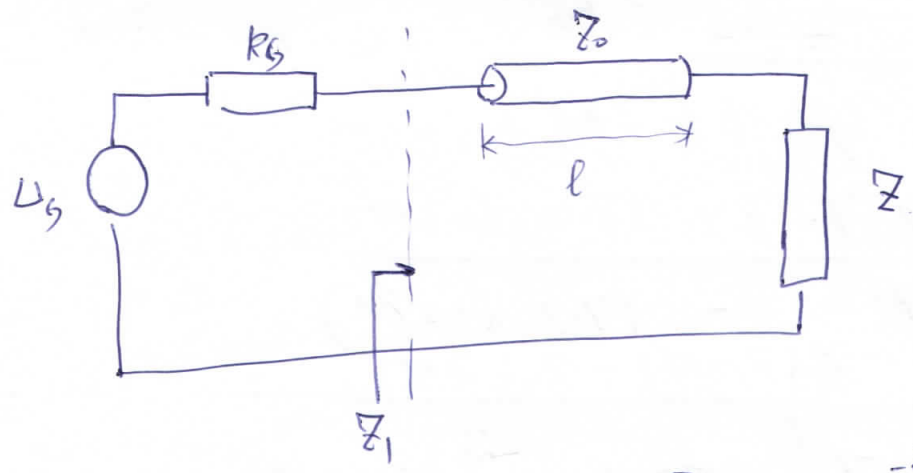
①  $x=l \rightarrow$

$$\hat{U}_+(l, p) = \hat{U}_+(0, p) e^{-p\sqrt{LC}l}$$

$$\hat{U}_-(l, p) = \hat{U}_-(0, p) e^{+p\sqrt{LC}l}$$

$$\rho_Z = \frac{\hat{U}_+(l, p)}{\hat{U}_-(l, p)} = \frac{Z - Z_0}{Z + Z_0}$$

$$\Rightarrow \frac{\hat{U}_-(0, p)}{\hat{U}_+(0, p)} = \frac{\hat{U}_-(l, p) e^{-p\sqrt{LC}l}}{\hat{U}_+(l, p) e^{+p\sqrt{LC}l}} = \rho_Z e^{-2p\sqrt{LC}l}$$



$$\begin{cases} \hat{U}(x,p) = \hat{U}_{+0} e^{-p\sqrt{L}x} + \hat{U}_{-0} e^{+p\sqrt{L}x} = \hat{U}_{+0} e^{-\gamma x} + \hat{U}_{-0} e^{\gamma x} \\ \hat{I}(x,p) = \hat{I}_{+0} e^{-p\sqrt{L}x} + \hat{I}_{-0} e^{+p\sqrt{L}x} = \hat{I}_{+0} e^{-\gamma x} + \hat{I}_{-0} e^{\gamma x} \end{cases}$$

Note that  $\frac{\hat{U}_{+0}}{\hat{I}_{+0}} = Z_0 = -\frac{\hat{U}_{-0}}{\hat{I}_{-0}}$

at  $x=l$ :

$$\begin{aligned} \hat{U}_l &= \hat{U}_{+0} e^{-\gamma l} + \hat{U}_{-0} e^{\gamma l} \\ \hat{I}_l &= \hat{I}_{+0} e^{-\gamma l} + \hat{I}_{-0} e^{\gamma l} = \frac{\hat{U}_{+0}}{Z_0} e^{-\gamma l} - \frac{\hat{U}_{-0}}{Z_0} e^{\gamma l} \end{aligned}$$

Note that  $\frac{\hat{U}_l}{\hat{I}_l} = Z \leftarrow \text{load.}$

$$\begin{aligned} Z_0 \hat{I}_l &= \hat{U}_{+0} e^{-\gamma l} - \hat{U}_{-0} e^{\gamma l} \\ \text{①+②: } \hat{U}_l + Z_0 \hat{I}_l &= 2\hat{U}_{+0} e^{-\gamma l} \Rightarrow \hat{U}_{+0} = \frac{1}{2} (\hat{U}_l + Z_0 \hat{I}_l) e^{\gamma l} \\ \text{①-②: } \hat{U}_l - Z_0 \hat{I}_l &= 2\hat{U}_{-0} e^{\gamma l} \Rightarrow \hat{U}_{-0} = \frac{1}{2} (\hat{U}_l - Z_0 \hat{I}_l) e^{-\gamma l} \\ \Rightarrow \hat{U}_{+0} &= \frac{1}{2} \hat{I}_l \left( \frac{\hat{U}_l}{\hat{I}_l} + Z_0 \right) e^{\gamma l} = \frac{1}{2} \hat{I}_l (Z + Z_0) e^{\gamma l} \\ \hat{U}_{-0} &= \frac{1}{2} \hat{I}_l (Z - Z_0) e^{-\gamma l} \end{aligned}$$

$$\Rightarrow \begin{cases} \hat{U}(x,p) = \frac{1}{2} \hat{I}_l (Z + Z_0) e^{\gamma(l-x)} + \frac{1}{2} \hat{I}_l (Z - Z_0) e^{-\gamma(l-x)} \\ \hat{I}(x,p) = \frac{1}{2} \hat{I}_l \frac{Z + Z_0}{Z_0} e^{\gamma(l-x)} - \frac{1}{2} \hat{I}_l \frac{Z - Z_0}{Z_0} e^{-\gamma(l-x)} \end{cases}$$

at  $x=0$ :

$$\begin{aligned} \hat{U}(0,p) &= \frac{1}{2} \hat{I}_l \left[ (Z + Z_0) e^{\gamma l} + (Z - Z_0) e^{-\gamma l} \right] \\ \hat{I}(0,p) &= \frac{1}{2} \frac{\hat{I}_l}{Z_0} \left[ (Z + Z_0) e^{\gamma l} - (Z - Z_0) e^{-\gamma l} \right] \end{aligned}$$

$$\begin{aligned}
 z_1 &= z_0 \frac{1 + \frac{z-z_0}{z+z_0} (1-2\gamma l)}{1 - \frac{z-z_0}{z+z_0} (1-2\gamma l)} \\
 &= z \frac{(z+z_0) + (z-z_0)(1-2\gamma l)}{(z+z_0) - (z-z_0)(1-2\gamma l)} \\
 &= z_0 \frac{z(2-2\gamma l) + z_0(2\gamma l)}{z(2+2\gamma l) + z_0(2\gamma l)} \\
 &= z_0 \frac{z(1-\gamma l) + z_0\gamma l}{z(1+\gamma l) + z_0(1+\gamma l)} \\
 &= z_0 \frac{z + \gamma l(z_0 - z)}{z_0 + \gamma l(z_0 + z)} \\
 &= z \frac{1 + \gamma l(z_0/z - 1)}{1 + \gamma l(1 + z/z_0)}
 \end{aligned}$$

$$\begin{aligned}
 z_1 &= z_0 \frac{1 + \gamma l z_0/z}{1 + \gamma l} \\
 &= \frac{z + \gamma l z_0}{1 + \gamma l} \rightarrow z_1 \approx z_0 \\
 &= z + p\sqrt{c} \cdot l \cdot \frac{z}{\sqrt{c}} \\
 &= z + p \cdot l
 \end{aligned}$$

$$z_1 = z \frac{1 - \gamma l}{1 + \gamma l z_0/z} = \frac{1 - \gamma l}{\frac{1}{z} + \gamma l/z_0}$$

$$\frac{p\sqrt{c} \cdot l}{\sqrt{c}} = p \cdot l$$

$$\frac{\hat{V}(0,p)}{\hat{I}(0,p)} = Z_1 = Z_0 \frac{(Z+Z_0)e^{pL} + (Z-Z_0)e^{-pL}}{(Z+Z_0)e^{pL} + (Z-Z_0)e^{-pL}}$$

$$= Z_0 \frac{1 + \frac{Z-Z_0}{Z+Z_0} e^{-2pL}}{1 - \frac{Z-Z_0}{Z+Z_0} e^{-2pL}}$$

$$\Rightarrow Z_1 = Z_0 \frac{1 + \beta_Z e^{-2p\sqrt{LC}l}}{1 - \beta_Z e^{-2p\sqrt{LC}l}} = Z_0 \frac{\cosh(p\sqrt{LC}l)}{\sinh(p\sqrt{LC}l)}$$

\* For open end,  $\beta_Z = \frac{Z-Z_0}{Z+Z_0} \xrightarrow{Z \rightarrow \infty} 1$

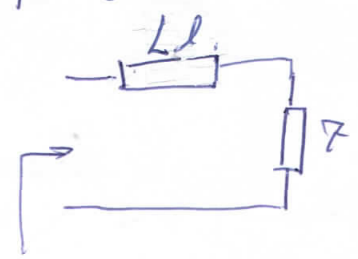
$$Z_1 = Z_0 \frac{1 + e^{-2p\sqrt{LC}l}}{1 - e^{-2p\sqrt{LC}l}} = Z_0 \frac{\cosh(p\sqrt{LC}l)}{\sinh(p\sqrt{LC}l)}$$

For  $p\sqrt{LC}l \ll 1$  ( $l \ll \lambda$ )

$$Z_1 \approx Z \frac{1 + p\sqrt{LC} \cdot l \cdot Z_0 - Z/Z_0}{1 - p\sqrt{LC} \cdot l \cdot Z - Z/Z_0}$$

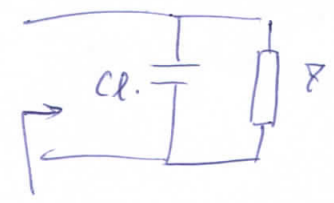
For  $Z \ll Z_0 = \sqrt{L/C} \cdot \sqrt{1/c}$

$Z_1 \approx Z + pLl \Rightarrow$  ~~of a series connect~~



For  $Z \gg Z_0$

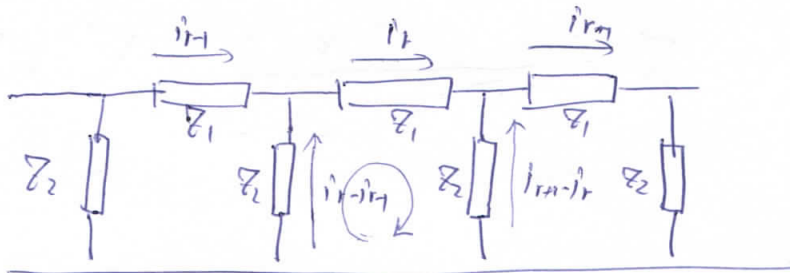
$$Z_1 \approx \frac{1}{1/Z + pC l}$$



# § 5.2 RLC Network (Sleep)

→ Transmission line → impracticable for creating rectangular pulses. ~~to~~ w/ a duration > 500ns

⇒ discrete RLC element.



$$-Z_2(i_r - i_{r-1}) - Z_1 i_r + Z_2(i_{r+1} - i_r) = 0$$

$$\Rightarrow i_r(-Z_2 - Z_1 - Z_2) + i_{r-1} Z_2 + i_{r+1} Z_2 = 0$$

$$\underline{i_r(Z_1 + 2Z_2) - i_{r-1} Z_2 - i_{r+1} Z_2 = 0}$$

Transfer function:  $\hat{G}$

Laplace transform  $\Rightarrow \hat{i}_r(Z_1 + 2Z_2) - \hat{i}_{r-1} Z_2 + \hat{i}_{r+1} Z_2 = 0$

Transfer funct:  $\hat{G} \Rightarrow \hat{i}_{r+1} = \hat{G} \hat{i}_r$

let  $p \rightarrow i\omega$  (Fourier)

$$\hat{G}(i\omega) = g(\omega) e^{i\phi(\omega)} = e^{a(\omega) + i\phi(\omega)}$$

$$\Rightarrow \hat{i}_r(Z_1 + 2Z_2) - \hat{i}_r e^{-(a+i\phi)} Z_2 - \hat{i}_r e^{a+i\phi} Z_2 = 0$$

$a(\omega) = \ln g(\omega)$

$$\hat{i}_r [Z_1 + 2Z_2 - Z_2 e^{-(a+i\phi)} - Z_2 e^{a+i\phi}] = 0$$

~~$Z_1 + 2Z_2$~~

$$Z_1 + 2Z_2 - 2Z_2 \cosh(a+i\phi) = 0$$

$$\frac{Z_1 + 2Z_2}{Z_2} = 2 \cosh(a+i\phi)$$

$$\Rightarrow 1 + \frac{Z_1}{2Z_2} = \cosh(a) \cosh(i\phi) + i \sinh(a) \sin(\phi)$$

1.  $g(\omega) = 1$ , i.e.  $a(\omega) = 0 \Rightarrow$  No amplitude reduction  
 shape of the pulse remains unchanged unless  $\phi(\omega) = k\omega$ .  
 $\Rightarrow$  delay chain.

2.  $\phi(\omega) = 0$ ,  $a(\omega) = \text{const} < 0 \Rightarrow$  frequency-independent  
 attenuation of the pulse.  
 $\Rightarrow$  ideal attenuator

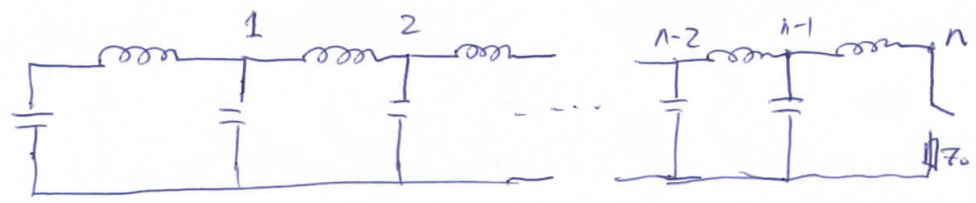
\* For a delay chain.  $(a(\omega) = 0) \Rightarrow \frac{Z_1}{2Z_2} = \cos(\phi)$

$$1 + \frac{Z_1}{2Z_2} = \cos(\phi) \Rightarrow -1 < \frac{Z_1}{2Z_2} < 0$$

$\uparrow$   
 Real & negative

$\Rightarrow$  Only combinations of capacitances and inductances are suitable elements for such a chain.

Ex:



$$-1 < \frac{\sum_1}{4 \sum_2} < 0, \quad \sum_1 = i\omega L, \quad \sum_2 = \frac{1}{i\omega C} \quad \leftarrow \begin{array}{l} \text{Fourier} \\ \text{Transform} \end{array} \quad p \text{ is}$$

$$\Rightarrow -1 < \frac{-\omega^2 LC}{4} < 0 \quad \Leftrightarrow \Rightarrow 1 > \frac{\omega^2 LC}{4} > 0$$

$$0 < \omega < \frac{2}{\sqrt{LC}} \quad \leftarrow \frac{4}{LC} > \omega^2 > 0$$

$$i_r [\sum_1 + 2\sum_2] - i_{r-1} \sum_2 - i_{r+1} \sum_2 = 0 \quad \frac{\sum_1 = pL, \quad \sum_2 = \frac{1}{pC}}{\text{Laplace}}$$

$$i_r \left( Lp + \frac{2}{pC} \right) - \frac{i_{r-1}}{pC} - \frac{i_{r+1}}{pC} = 0$$

$$\hat{i}_r = A e^{r\theta} + B e^{-r\theta} \quad \text{where } \theta = i\phi(\omega)$$

Fourier transform forward

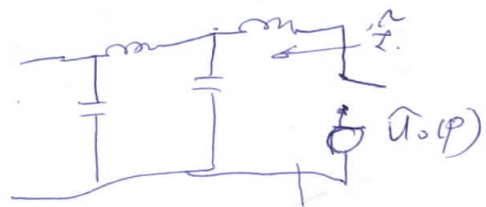
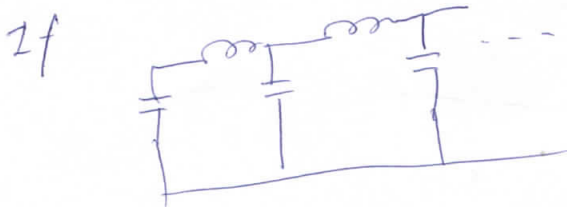
~~$$\cosh(i\phi) = \cosh(\theta) = \frac{\sum_1 + 2\sum_2}{\sum_2} = \frac{pL + \frac{2}{pC}}{\frac{1}{pC}} = 2$$~~

$$\cosh[a + r\theta] = \cosh(i\phi) = \cosh\theta$$

$$\begin{aligned} \because a=0 \text{ for delay chain.} \\ \Rightarrow 1 + \frac{\sum_1}{2\sum_2} &= \frac{1}{2} \frac{\sum_1 + 2\sum_2}{\sum_2} = 1 + \frac{\sum_1}{2\sum_2} = 1 + \frac{pL}{2/pC} \\ &= 1 + \frac{LC}{2} p^2 \end{aligned}$$

$$1 + \frac{\sum_1}{2\sum_2} = \cosh(\phi)$$

A, B  $\rightarrow$  determined from the Boundary. @ 1<sup>st</sup> & last mesh.

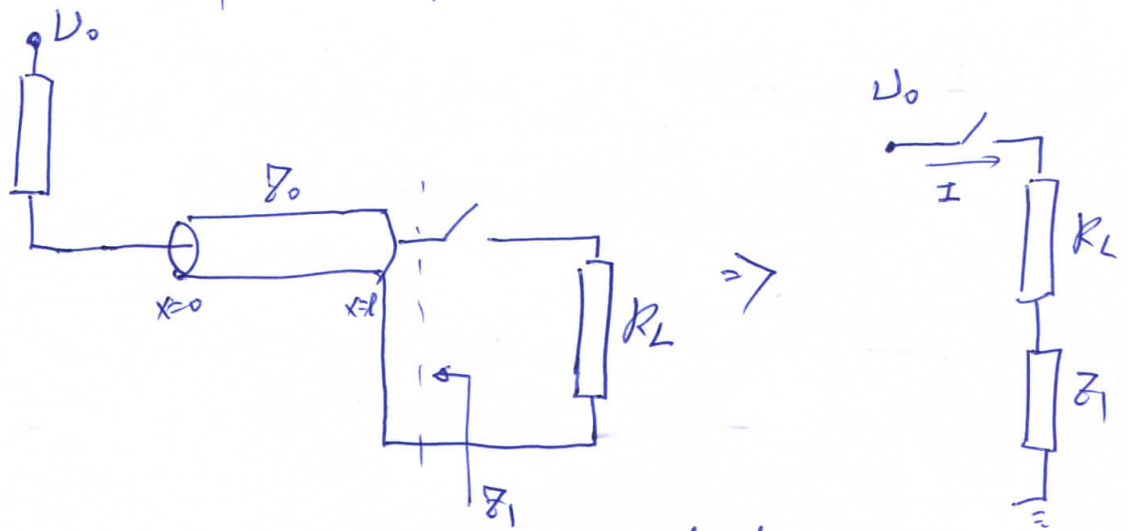


$$\hat{i}_n(p) =$$

skip



7.5.1.4 Example:

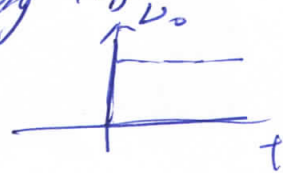


Look back to the source from the load,

$$Z_1 \approx Z_0 \frac{\cosh(p\sqrt{LC}l)}{\sinh(p\sqrt{LC}l)} = Z_0 \coth(p\sqrt{LC}l)$$

Assuming the impedance of the source is very large  $\Rightarrow$  open circuit.

Assuming  $U_0 = U_0 H(t)$



$\Rightarrow$  Laplace:  $\hat{U} = \frac{U_0}{p}$ ,  $Z = R_L + Z_1$ ,  $T = \sqrt{LC}l$

$$\hat{I} = \frac{\hat{U}}{Z} = \frac{U_0}{p} \frac{1}{R_L + Z_0 \coth(pT)} = \frac{U_0}{p} \frac{1}{R_L + Z_0 \frac{e^{pT} + e^{-pT}}{e^{pT} - e^{-pT}}}$$

~~$$= \frac{U_0}{p(R_L + Z_0)} \frac{R_L + Z_0}{R_L + Z_0} + \frac{Z_0}{R_L + Z_0} \coth(pT) = \frac{U_0}{p} \frac{1}{R_L e^{pT} - R_L e^{-pT} + Z_0 e^{pT} + Z_0 e^{-pT}}$$~~

~~$$\frac{U_0}{p(R_L + Z_0)}$$~~

$$= \frac{U_0}{p} \frac{1 - e^{-2pT}}{(R_L + Z_0) + (Z_0 - R_L) e^{-2pT}}$$

$$= \frac{U_0}{p(R_L + Z_0)} \frac{1 - e^{-2pT}}{1 + \left(\frac{Z_0 - R_L}{Z_0 + R_L}\right) e^{-2pT}}$$

$$f(x) = \frac{1}{1+x} \quad f(0) = 1$$

$$f'(x) = -\frac{1}{(1+x)^2} \quad f'(0) = -1$$

$$f''(x) = 2! \frac{1}{(1+x)^3} \quad f''(0) = 2!$$

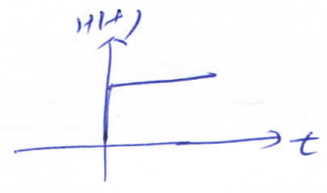
$$f^{(3)}(x) = -3! \frac{1}{(1+x)^4} \quad f^{(3)}(0) = -3!$$

$$\frac{1}{1+x} = 1 - x + \frac{2!}{2!} x^2 - \frac{3!}{3!} x^3 + \dots$$

$$= 1 - x + x^2 - x^3 + \dots$$

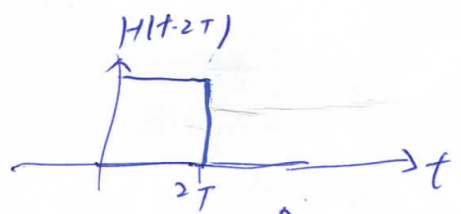
$$\Rightarrow \hat{I} \approx \frac{U_0 (1 - e^{-2pT})}{p(R_L + Z_0)} \left[ 1 - \left( \frac{Z_0 - R_L}{Z_0 + R_L} \right) e^{-2pT} + \left( \frac{Z_0 - R_L}{Z_0 + R_L} \right)^2 e^{-4pT} - \dots \right]$$

Inverse Laplace:  $\mathcal{L}^{-1} \left\{ \frac{1}{p} \right\} = H(t)$

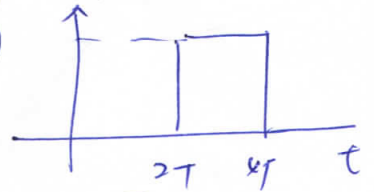


$$\mathcal{L}^{-1} \left\{ \frac{e^{-ap}}{p} \right\} = H(t-a)$$

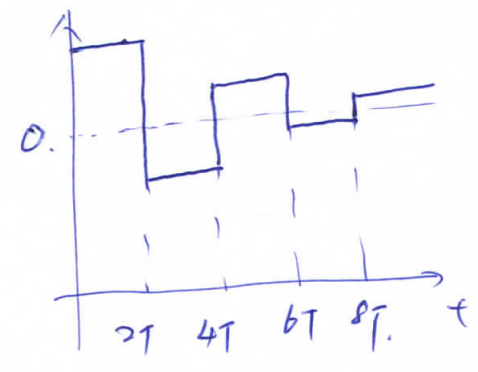
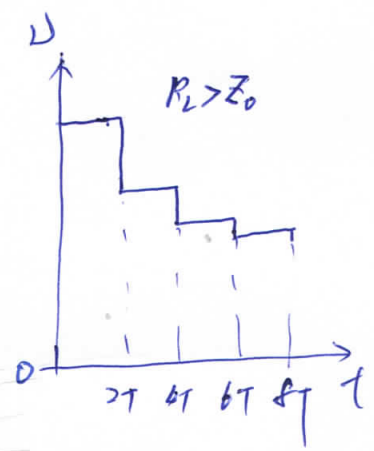
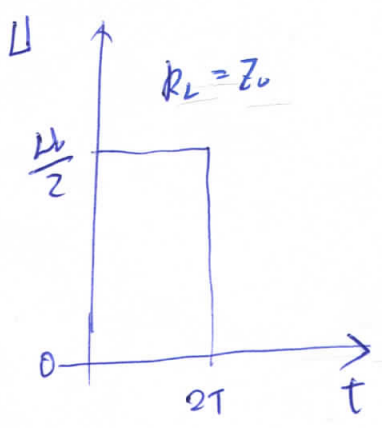
$$\Rightarrow \mathcal{L}^{-1} \left\{ \frac{1 - e^{-2pT}}{p} \right\} = 1 - H(t-2T)$$



$$\mathcal{L}^{-1} \left\{ \frac{e^{-2pT} - e^{-4pT}}{p} \right\} = H(t-2T) - H(t-4T)$$



$$\Rightarrow I = \frac{U_0}{Z_0 + R_L} \left\{ \left[ 1 - H(t-2T) \right] - \frac{Z_0 - R_L}{Z_0 + R_L} \left[ H(t-2T) - H(t-4T) \right] + \frac{Z_0 - R_L}{Z_0 + R_L} \left[ H(t-4T) - H(t-6T) \right] - \dots \right\}$$



## Q 6. Pulse Transmission and Transformation 12/21

### Q 6.1 Self-Magnetic Insulation in Vacuum Lines

→ Some tasks in science & technology required brightness of intense pulsed radiation  $> 100 \text{ TW/cm}^2 \cdot \text{sr}$ .

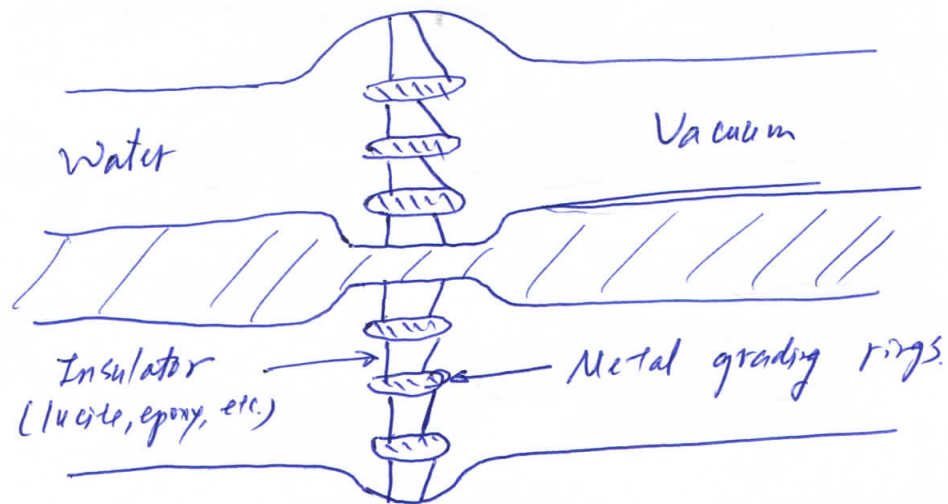
w)  $E > 1 \text{ MJ}$ .

⇒ Electric power  $> 100 \text{ TW}$

( $\rho$  - density  $> 100 \text{ TW/m}^2$  needed)  
Flux

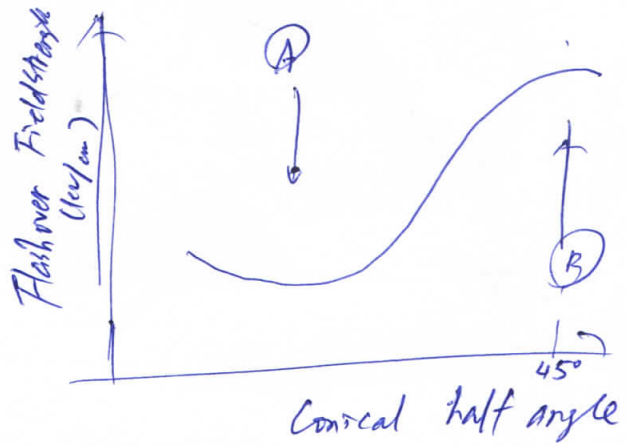
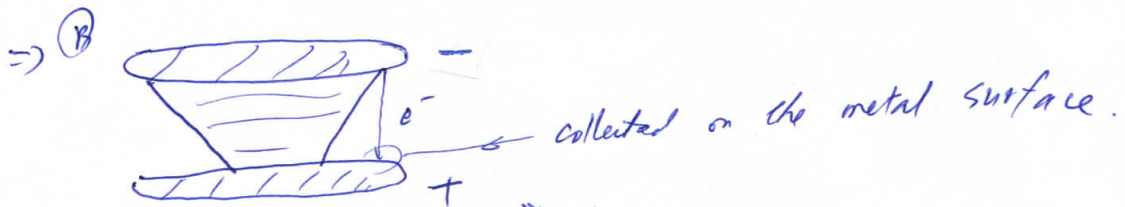
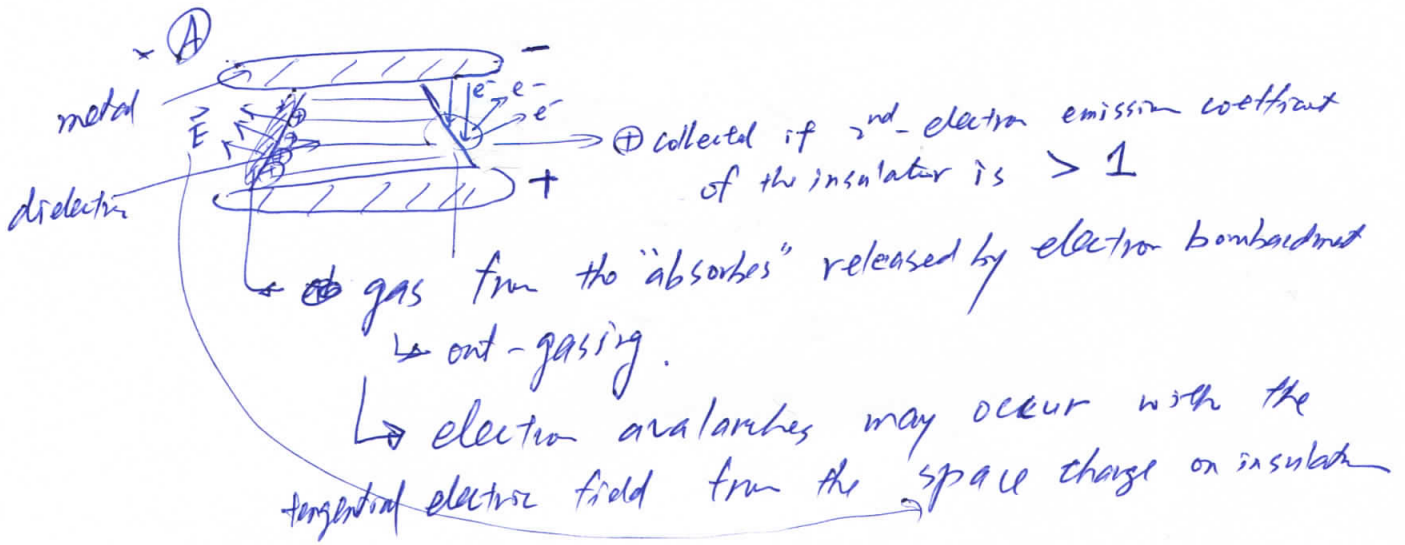
⇒ Vacuum environment is required.

⇒ HV pulse must enter a vacuum vessel hosting the source through an insulating interface separating the liquid dielectric from the vacuum section.



- \* The interface consists of insulating rings separated by metallic grading rings.
- \* The metal & dielectric rings are sealed to hold the high vacuum either by O-rings or by metal-to-dielectric bond.
- \* Sparking on the surface of on the vacuum side is more important.

\* Electrons may be produced by field emission on metallic surfaces.



\* Dielectric-vacuum ~~surface~~ interface is the weakest element of a high-voltage pulse line under electric-field stress.

$$E_{DB} = \frac{7 \times 10^5}{t^{1/6} A^{1/10}} \text{ (V/m)}$$

$\leftarrow$  time when  $E > 87\% E_{max}$

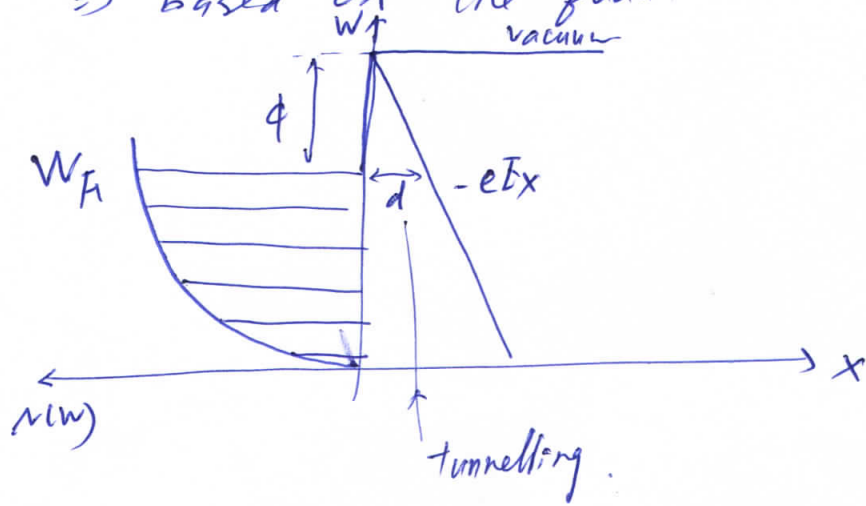
for  $t = 10 \text{ ns}$ ,  $E_{max} = 20 \text{ MV/m} \Rightarrow P < 1 \text{ TW/m}^2$

# § 6.1.1 Vacuum Breakdown on Metallic Surfaces <sup>P123</sup>

\* For  $E \gg 20 \text{ MV/m}$ , explosive electron emission with plasma formation occurs on ~~metal~~ metallic surfaces in vacuum.

⇒ unlimited electron source w/ zero work function.

⇒ based on the quantum mechanical tunnelling effect.



$$j = \frac{1.54 \times 10^{-6} \beta^2 E^2}{\phi} \exp \left\{ - \frac{6.83 \times 10^7 \phi^{3/2} \theta(y)}{\beta E} \right\}$$

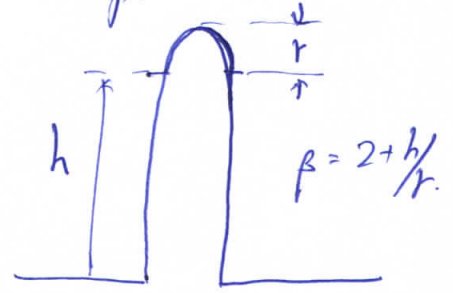
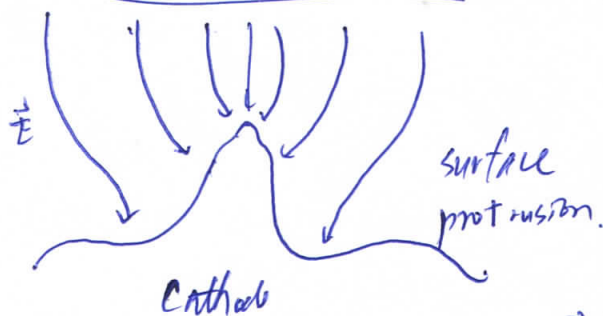
$\theta(y) \approx 0.956 - 1.06 y^2$   
 $y = 3.8 \times 10^{-4} \frac{\sqrt{E}}{\phi}$

$\beta E \propto \sqrt{E}$   
 $\propto \sqrt{E}$   
 field enhance factor.

$\phi$  ← work function eV.

\* Calculated current density is  $\ll$  observed experimentally.

⇒ whisker model. ∴ "whisker" is a fine filamentary metallic protrusion.



⇒  $\beta = 100$  is needed but  $h/r \sim 100$  is not observed.

- \* Dielectric inclusions are involved in the emission centres. 1974
- ⇒ tunnelling current from the metal into the dielectric ~~is now~~ plays a dominated role.
- \* current flowing through the emission sites ⇒ strong heating & vaporises the sites ⇒ ionised by succeeding  $e^-$ .

## 76.1.2. Qualitative Description of Self-Magnetic Insulation

- \*  $E \gg 20 \text{ MV/m}$  ⇒ homogeneous plasma layer generated within a few ns.

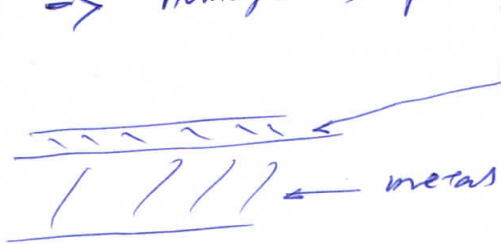


(Fig 6.5)

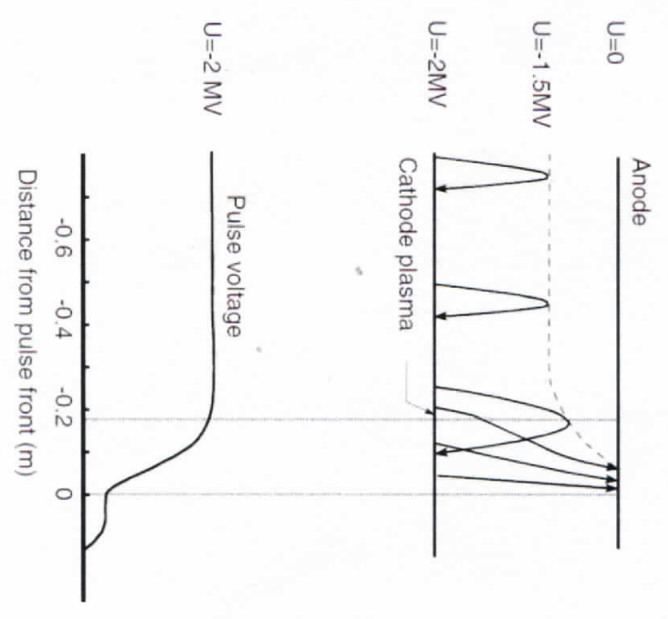
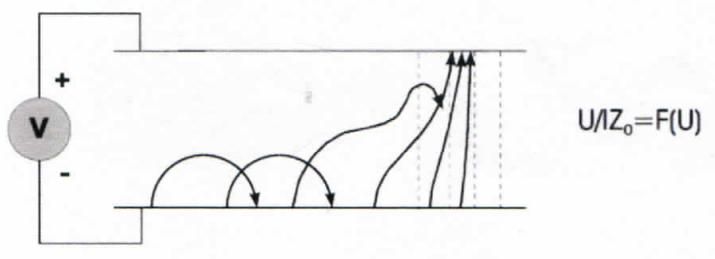
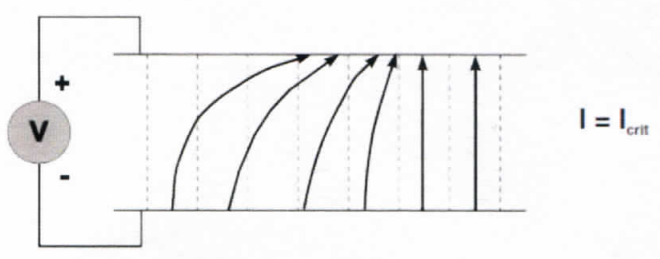
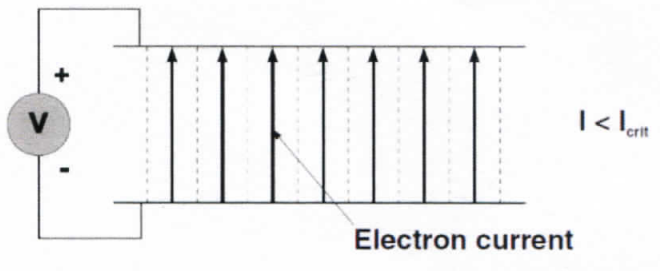
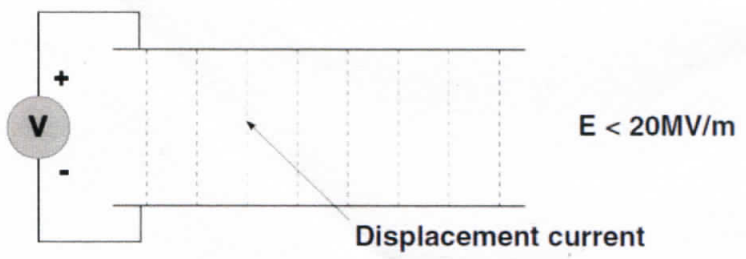
⇒ Before breakdown → displace current

- \*  $I < I_{crit}$
  - $I = I_{crit}$
  - $I > I_{crit}$
- electrons are deflected by the self-magnetic field of the total line current.

⇒ electrons orbits can no longer reach the anode.  
 ⇒ more & more sections are insulated  
 ⇒ An electron sheath forms on the negative conductor ⇒ impedance

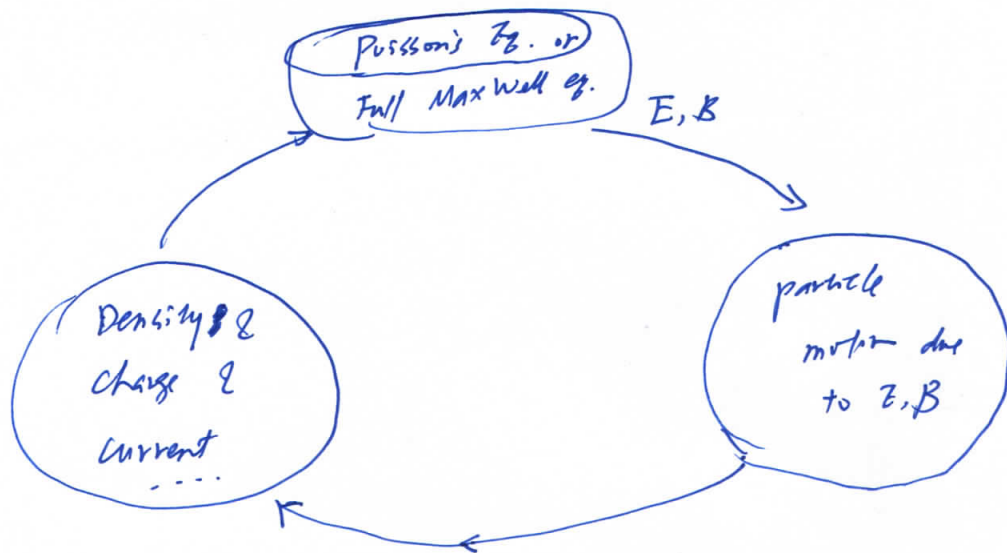
≠ vacuum impedance.  
 ⇒ electromagnetic shock wave is formed.

- \* (Fig 6.6) As long as the voltage ramp remains below the breakdown threshold, the wave propagates at the speed of light.

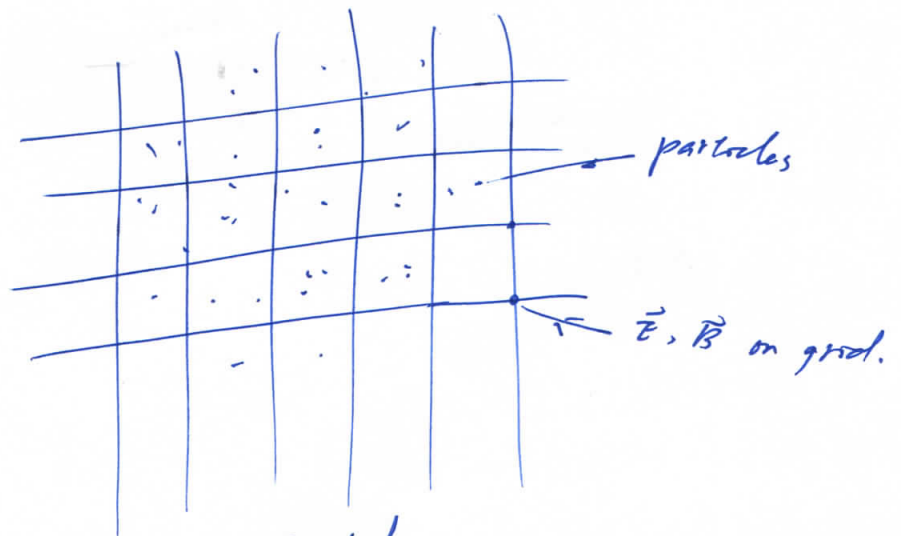


### § 6.1.3 Quantitative Description of Self-Magnetic Insulation p126

- \* Maxwell's field equations simultaneously w/ the Hamiltonian equations of motion are needed.
- \* They are solved ~~numerically~~ numerically using particle-in-cell (PIC) method.



### § 6.1.3.1 An



### § 6.1.3.1 Analytical Models.

- \* Model for stationary conditions at a large distance behind the loss front of the wave.
- ⇒ only a net current flow  $j_z$  in the  $z$ -direction.
- Assume a homogeneous coaxial line.



Maxwell's eq:

$$\begin{cases} \nabla \cdot \vec{E} = \frac{\rho}{\epsilon_0} \\ \nabla \cdot \vec{B} = 0 \end{cases} \quad , \quad \begin{cases} \nabla \times \vec{E} = - \frac{\partial \vec{B}}{\partial t} \\ \nabla \times \vec{B} = \mu_0 \vec{j} + \mu_0 \epsilon_0 \frac{\partial \vec{E}}{\partial t} \end{cases}$$

$$\nabla \cdot \vec{B} = 0 \Rightarrow \vec{B} \equiv \nabla \times \vec{A}$$

$$\nabla \times \vec{E} = - \frac{\partial \vec{B}}{\partial t} \Rightarrow \nabla \times \vec{E} = - \frac{\partial}{\partial t} \nabla \times \vec{A} \Rightarrow \nabla \times \left( \vec{E} + \frac{\partial \vec{A}}{\partial t} \right) = 0$$

$$\Rightarrow \vec{E} + \frac{\partial \vec{A}}{\partial t} = - \nabla \phi$$

$$\Rightarrow \vec{E} \equiv - \nabla \phi - \frac{\partial \vec{A}}{\partial t}$$

$$\nabla \cdot \vec{E} = \frac{\rho}{\epsilon_0} \Rightarrow \nabla \cdot \left( - \nabla \phi - \frac{\partial \vec{A}}{\partial t} \right) = \frac{\rho}{\epsilon_0}$$

$$\nabla^2 \phi + \frac{\partial}{\partial t} (\nabla \cdot \vec{A}) = - \frac{\rho}{\epsilon_0}$$

$$\nabla \times \vec{B} = \mu_0 \vec{j} + \mu_0 \epsilon_0 \frac{\partial \vec{E}}{\partial t}$$

$$\Rightarrow \nabla \times (\nabla \times \vec{A}) = \mu_0 \vec{j} + \mu_0 \epsilon_0 \frac{\partial}{\partial t} \left( - \nabla \phi - \frac{\partial \vec{A}}{\partial t} \right)$$

$$\nabla (\nabla \cdot \vec{A}) - \nabla^2 \vec{A} = \mu_0 \vec{j} - \nabla \left( \mu_0 \epsilon_0 \frac{\partial \phi}{\partial t} \right) - \mu_0 \epsilon_0 \frac{\partial^2 \vec{A}}{\partial t^2}$$

$$\Rightarrow \left( \nabla^2 \vec{A} - \mu_0 \epsilon_0 \frac{\partial^2 \vec{A}}{\partial t^2} \right) - \nabla \left( \nabla \cdot \vec{A} + \mu_0 \epsilon_0 \frac{\partial \phi}{\partial t} \right) = - \mu_0 \vec{j}$$

All you need for Maxwell's eq.

\* The coulomb gauge:  $\nabla \cdot \vec{A} = 0$

$$\nabla^2 \phi + \frac{\partial}{\partial t} (\nabla \cdot \vec{A}) = \frac{\rho}{\epsilon_0} \Rightarrow \nabla^2 \phi = - \frac{\rho}{\epsilon_0}$$

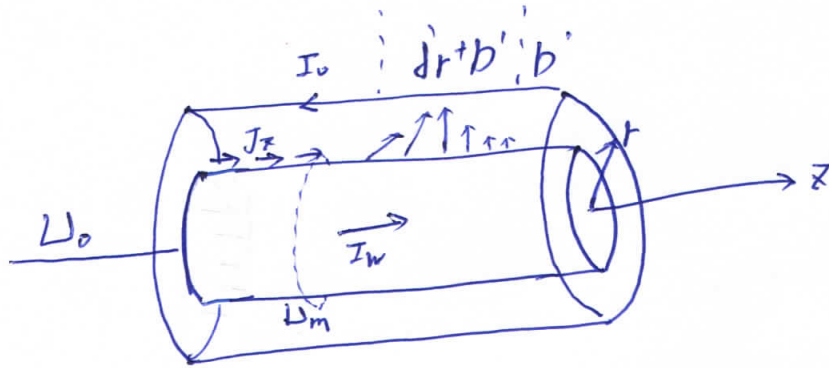
$$\left( \nabla^2 \vec{A} - \mu_0 \epsilon_0 \frac{\partial^2 \vec{A}}{\partial t^2} \right) - \nabla \left( \nabla \cdot \vec{A} + \mu_0 \epsilon_0 \frac{\partial \phi}{\partial t} \right) = - \mu_0 \vec{j} \Rightarrow \nabla^2 \vec{A} - \mu_0 \epsilon_0 \frac{\partial^2 \vec{A}}{\partial t^2} = - \mu_0 \vec{j} + \mu_0 \epsilon_0 \nabla \left( \frac{\partial \phi}{\partial t} \right)$$

Lorentz gauge:  $\nabla \cdot \vec{A} = -\mu_0 \epsilon_0 \frac{\partial \phi}{\partial t}$

1128

$$\nabla^2 \phi + \frac{1}{c^2} (\nabla \cdot \vec{A}) = -\frac{\rho}{\epsilon_0} \Rightarrow \nabla^2 \phi - \mu_0 \epsilon_0 \frac{\partial^2 \phi}{\partial t^2} = -\frac{\rho}{\epsilon_0}$$

$$\left( \nabla^2 \vec{A} - \mu_0 \epsilon_0 \frac{\partial^2 \vec{A}}{\partial t^2} \right) - \nabla (\nabla \cdot \vec{A} + \mu_0 \epsilon_0 \frac{\partial \phi}{\partial t}) = -\mu_0 \vec{j} \Rightarrow \nabla^2 \vec{A} - \mu_0 \epsilon_0 \frac{\partial^2 \vec{A}}{\partial t^2} = -\mu_0 \vec{j}$$



Stationary condition:  $\frac{\partial}{\partial t} = 0$

$$\nabla^2 \vec{A} = \mu_0 \epsilon_0 \frac{\partial^2 \vec{A}}{\partial t^2} - \mu_0 \vec{j} \Rightarrow -\mu_0 \vec{j}$$

$$\nabla^2 \phi = \mu_0 \epsilon_0 \frac{\partial^2 \phi}{\partial t^2} - \frac{\rho}{\epsilon_0} \Rightarrow -\frac{\rho}{\epsilon_0}$$

In cylindrical:  $\nabla^2 = \frac{1}{r} \frac{\partial}{\partial r} \left( r \frac{\partial}{\partial r} \right) + \frac{1}{r^2} \frac{\partial^2}{\partial \phi^2} + \frac{\partial^2}{\partial z^2}$

$$\left( \nabla^2 \vec{A} \right)_z = \nabla^2 A_z$$

$$\Rightarrow \begin{cases} \frac{1}{r} \frac{\partial}{\partial r} \left( r \frac{\partial A_z}{\partial r} \right) = -\mu_0 j_z \\ \frac{1}{r} \frac{\partial}{\partial r} \left( r \frac{\partial \phi}{\partial r} \right) = -\frac{\rho}{\epsilon_0} \end{cases}$$

Momentum conservation:  $p_z = \gamma m_0 \dot{z} - e A_z = 0$

Energy conservation:  $\gamma m_0 c^2 - e \phi = m_0 c^2$

$$\beta = \frac{v}{c}, \quad \gamma = \frac{1}{\sqrt{1-\beta^2}} = 1 + \frac{e \phi}{m_0 c^2}$$

↑  
relativistic factor